

# pH-dependent Inhibition of Voltage-gated H<sup>+</sup> Currents in Rat Alveolar Epithelial Cells by Zn<sup>2+</sup> and Other Divalent Cations

Vladimir V. Cherny and Thomas E. DeCoursey

From the Department of Molecular Biophysics and Physiology, Rush Presbyterian St. Luke's Medical Center, Chicago, Illinois 60612

**abstract** Inhibition by polyvalent cations is a defining characteristic of voltage-gated proton channels. The mechanism of this inhibition was studied in rat alveolar epithelial cells using tight-seal voltage clamp techniques. Metal concentrations were corrected for measured binding to buffers. Externally applied ZnCl<sub>2</sub> reduced the H<sup>+</sup> current, shifted the voltage-activation curve toward positive potentials, and slowed the turn-on of H<sup>+</sup> current upon depolarization more than could be accounted for by a simple voltage shift, with minimal effects on the closing rate. The effects of Zn<sup>2+</sup> were inconsistent with classical voltage-dependent block in which Zn<sup>2+</sup> binds within the membrane voltage field. Instead, Zn<sup>2+</sup> binds to superficial sites on the channel and modulates gating. The effects of extracellular Zn<sup>2+</sup> were strongly pH<sub>o</sub> dependent but were insensitive to pH<sub>i</sub>, suggesting that protons and Zn<sup>2+</sup> compete for external sites on H<sup>+</sup> channels. The apparent potency of Zn<sup>2+</sup> in slowing activation was ~10× greater at pH<sub>o</sub> 7 than at pH<sub>o</sub> 6, and ~100× greater at pH<sub>o</sub> 6 than at pH<sub>o</sub> 5. The pH<sub>o</sub> dependence suggests that Zn<sup>2+</sup>, not ZnOH<sup>+</sup>, is the active species. Evidently, the Zn<sup>2+</sup> receptor is formed by multiple groups, protonation of any of which inhibits Zn<sup>2+</sup> binding. The external receptor bound H<sup>+</sup> and Zn<sup>2+</sup> with pK<sub>a</sub> 6.2–6.6 and pK<sub>M</sub> 6.5, as described by several models. Zn<sup>2+</sup> effects on the proton chord conductance–voltage (g<sub>H</sub>–V) relationship indicated higher affinities, pK<sub>a</sub> 7 and pK<sub>M</sub> 8. CdCl<sub>2</sub> had similar effects as ZnCl<sub>2</sub> and competed with H<sup>+</sup>, but had lower affinity. Zn<sup>2+</sup> applied internally via the pipette solution or to inside-out patches had comparatively small effects, but at high concentrations reduced H<sup>+</sup> currents and slowed channel closing. Thus, external and internal zinc-binding sites are different. The external Zn<sup>2+</sup> receptor may be the same modulatory protonation site(s) at which pH<sub>o</sub> regulates H<sup>+</sup> channel gating.

**key words:** metal binding constants • cadmium • pH • hydrogen ion • ion channels

## INTRODUCTION

Voltage-gated proton channels differ from other voltage-gated ion channels, not only in their extreme selectivity for H<sup>+</sup>, but also in the regulation of their gating by pH<sub>o</sub> and pH<sub>i</sub>. The mechanism of permeation is believed to differ radically from traditional ion channels, which comprise water-filled pores through which ions diffuse: proton channels appear to conduct H<sup>+</sup> by a Grothuss-like mechanism of hopping across a hydrogen-bonded chain spanning the membrane (DeCoursey and Cherny, 1994, 1995, 1997, 1998; Cherny et al., 1995). If ion channels are defined narrowly as water-filled pores, then proton channels are not ion channels, although they conduct protons passively down their electrochemical gradient, and independently of other ionic species. In spite of these fundamental differences, it is remarkable how closely proton channels resemble other voltage-gated channels. H<sup>+</sup> channels activate upon depolarization with a sigmoidal time

course, deactivate exponentially, and exhibit a Cole-Moore effect (DeCoursey and Cherny, 1994) practically indistinguishable from the behavior of delayed rectifier K<sup>+</sup> channels (Cole and Moore, 1960). Low pH<sub>o</sub> shifts the voltage-activation curves of both H<sup>+</sup> channels and other ion channels toward positive potentials and slows activation at a given voltage. Voltage-gated proton channels characteristically are inhibited by extracellular polyvalent cations. The transition metals Zn<sup>2+</sup> and Cd<sup>2+</sup> have been used most frequently (Thomas and Meech, 1982; Byerly et al., 1984; Barish and Baud, 1984; Mahaut-Smith, 1989; DeCoursey, 1991; Kapus et al., 1993; Demaurex et al., 1993; DeCoursey and Cherny, 1993; Humez et al., 1995; Gordienko et al., 1996; Nordström et al., 1995), but Cu<sup>2+</sup>, Ni<sup>2+</sup>, Co<sup>2+</sup>, Hg<sup>2+</sup>, Be<sup>2+</sup>, Mn<sup>2+</sup>, Al<sup>3+</sup>, and La<sup>3+</sup> have similar effects (Thomas and Meech, 1982; Meech and Thomas, 1987; Byerly and Suen, 1989; Bernheim et al., 1993; DeCoursey and Cherny, 1994; Eder et al., 1995). To the extent that each has been explored, all of these metal cations shift the voltage dependence of activation (channel opening) to more positive potentials and slow the opening rate (Byerly et al., 1984; Barish and Baud, 1984; Meech and Thomas, 1987; Mahaut-Smith, 1989; DeCoursey, 1991; DeCoursey and Cherny, 1993; Demaurex et al., 1993; Kapus et al., 1993; Nordström et

Portions of this work were previously published in abstract form (DeCoursey, T.E., and V.V. Cherny. 1999. *Biophys. J.* 76:A147).

Address correspondence to Tom DeCoursey, Department of Molecular Biophysics and Physiology, Rush Presbyterian St. Luke's Medical Center, 1653 West Congress Parkway, Chicago, IL 60612. Fax: 312-942-8711; E-mail: tdecours@rush.edu

al., 1995; Gordienko et al., 1996). These effects resemble those of polyvalent cations on other ion channels (e.g., Frankenhaeuser and Hodgkin, 1957; Hille, 1968; Stanfield, 1975; Gilly and Armstrong, 1982; Spires and Begenisich, 1992, 1995; Arkett et al., 1994). Closer examination reveals differences, however. The H<sup>+</sup> channel is much more sensitive to external ZnCl<sub>2</sub> than are voltage-gated K<sup>+</sup> channels, which require 1,000-fold higher concentrations to produce comparable effects in squid (Spires and Begenisich, 1992), 10–100-fold higher concentrations in frog skeletal muscle (Stanfield, 1975), and 100-fold higher concentrations in *Shaker* (Spires and Begenisich, 1994). In addition, the effects of ZnCl<sub>2</sub> on squid axon K<sup>+</sup> channels are similar for addition to either side of the membrane and internally applied ZnCl<sub>2</sub> is quite potent (Begenisich and Lynch, 1974). In contrast, we find that ZnCl<sub>2</sub> has qualitatively different effects on H<sup>+</sup> channels depending on the side of application and thus binds to distinct external and internal sites.

The effects of metal cations on H<sup>+</sup> currents have been characterized variously as voltage-dependent block, voltage shifts induced by electrostatic effects on the voltage sensor, and specific binding to the channel. These interpretations invoke different mechanisms. Voltage-dependent block suggests that the metal ion enters the channel and crosses part of the membrane potential field to reach its block site in the pore. Here we explore the effects of ZnCl<sub>2</sub>, one of the more potent inhibitors of H<sup>+</sup> channels, as a prototypical metal inhibitor. We find that voltage-dependent block is not a viable mechanism. Prominent effects of Zn<sup>2+</sup> reflect specific binding that allosterically alters gating.

A key feature of the inhibition of H<sup>+</sup> currents by Zn<sup>2+</sup> is a profound pH dependence, which has not been described previously. Lowering pH<sub>o</sub> decreases the effectiveness of ZnCl<sub>2</sub>. Competition between Zn<sup>2+</sup> and H<sup>+</sup> has been noted previously for other channels, including Cl<sup>-</sup> (Hutter and Warner, 1967; Spalding et al., 1990; Rychkov et al., 1997) and K<sup>+</sup> (Spires and Begenisich, 1992, 1994). We consider whether the pH<sub>o</sub> dependence indicates that (a) the active form is not Zn<sup>2+</sup> but ZnOH<sup>+</sup>, (b) Zn<sup>2+</sup> and H<sup>+</sup> compete for the same binding site, or (c) there is noncompetitive inhibition; i.e., protonated channels have a lower affinity for Zn<sup>2+</sup>. We conclude that the external Zn<sup>2+</sup> receptor is formed by three or more protonation sites, perhaps comprising His residues, that together coordinate one Zn<sup>2+</sup>.

## MATERIALS AND METHODS

### Rat Alveolar Epithelial Cells

Type II alveolar epithelial cells were isolated from adult male Sprague-Dawley rats using enzyme digestion, lectin agglutination, and differential adherence, as described in detail elsewhere (DeCoursey et al., 1988; DeCoursey, 1990), with the exception

that we now use elastase without trypsin to dissociate the cells. The rats were anesthetized using sodium pentobarbital. In brief, the lungs were lavaged to remove macrophages, elastase was instilled, and then the tissue was minced and forced through fine gauze. Lectin agglutination and differential adherence further removed contaminating cell types. The preparation at first includes mainly type II alveolar epithelial cells, but after several days in culture the properties of the cells are more like type I cells. H<sup>+</sup> currents were studied in approximately spherical cells up to several weeks after isolation.

### Solutions

Solutions contained 100 mM buffer supplemented with tetramethylammonium (TMA) methanesulfonate (TMAMeSO<sub>3</sub>) to bring the osmolarity to ~300 mOsm. One exception was the pH<sub>o</sub> 7.0 solution made with 70 mM PIPES. External solutions contained 2 mM CaCl<sub>2</sub> or 2 mM MgCl<sub>2</sub>. Internal solutions contained 2 mM MgCl<sub>2</sub> and 1 mM EGTA. Solutions were titrated to the desired pH with TMA hydroxide (TMAOH) or methanesulfonic acid (solutions using BisTris as a buffer). A stock solution of TMAMeSO<sub>3</sub> was made by neutralizing TMAOH with methanesulfonic acid. TPEN (*N,N,N',N'*-tetrakis(2-pyridylmethyl)ethylenediamine) was purchased from Sigma Chemical Co.

### Buffers and Their Metal Binding Properties

The following buffers were used near their negative logarithm of the acid dissociation constant ( $pK_a$ ) (at 20°C) for measurements at the following pH: pH 5.0, Homopipes (homopiperazine-*N,N'*-bis-2-(ethanesulfonic acid),  $pK_a$  4.61); pH 5.5–6.0 Mes ( $pK_a$  6.15); pH 6.5 BisTris (bis[2-hydroxyethyl]imino-tris[hydroxymethyl]methane,  $pK_a$  6.50); pH 7.0 PIPES ( $pK_a$  6.80); pH 7.5–8.0 HEPES ( $pK_a$  7.55). Buffers were purchased from Sigma Chemical Co., except for Homopipes (Research Organics). Buffers such as Tricine and BES that reportedly complex strongly with transition metals (Good et al., 1966) were avoided. We could not find information in the literature on the Zn<sup>2+</sup> or Cd<sup>2+</sup> binding properties of the buffers used. Therefore, we measured the binding constants for a number of buffers, according to the method described by Good et al. (1966). This consisted of titrating the buffer alone, and then together with an equimolar amount of the metal salt (usually 10 mmol in a 100-ml vol). The binding constant was calculated from the relationship (Eq. 1):

$$K'_M = \frac{2\left(\frac{[H^+_M]}{K_a} - 1\right)}{[B]\left(\frac{K_a}{[H^+_M]} + 1\right)}, \quad (1)$$

where  $K'_M$  is the metal binding constant,  $K_a$  is the proton dissociation constant defined in Scheme III ( $-pK_a$  value),  $[H^+_M]$  is the H<sup>+</sup> concentration at the midpoint of the titration curve in the presence of the metal being tested and  $[B]$  is the total buffer concentration. The higher the affinity of the buffer for metal, the greater the shift in the titration curve. Table I gives the results.

Good et al. (1966) reported that the affinity of several buffers for Ca<sup>2+</sup> was generally about five log units weaker than that for Cu<sup>2+</sup>. A notable exception is Mes, which binds Ca<sup>2+</sup> weakly but Cu<sup>2+</sup> negligibly (Good et al., 1966). We find that Zn<sup>2+</sup> is bound roughly two log units more weakly than Cu<sup>2+</sup>, consistent with the lower affinity binding of Zn<sup>2+</sup> than Cu<sup>2+</sup> to various ionizable groups on proteins (Breslow, 1973). One exception to this rule is that PIPES did bind Zn<sup>2+</sup> weakly, whereas Cu<sup>2+</sup> was bound negligibly (Good et al., 1966). All buffers bound Cd<sup>2+</sup> detectably and to roughly the same extent that they bound Zn<sup>2+</sup>. It should be noted

TABLE I  
Affinity Constants of Buffers for Divalent Metals at 20°C

Buffer	$pK_a$ at 20°C	Metal binding constant ( $\log K'_M$ )				
	Measured (nominal)	Cu <sup>2+</sup>	Zn <sup>2+</sup>	Cd <sup>2+</sup>	Ca <sup>2+</sup>	Ni <sup>2+</sup>
Homopipes	4.51 ± 0.04 (8) [4.61]	—	0.8 (2)	0.9 (3)	NS (1)	0.2 (2)
Mes	6.23 ± 0.05 (7) [6.15]	— NS*	0.8 (2)	1.2 (2)	NS 0.7*	0.4 (2)
BisTris	6.52 ± 0.06 (8) [6.46]	—	2.2 (2)	1.9 (2)	2.0 (2)	3.3 (2)
PIPES	6.96 <sup>†</sup> ± 0.07 (10) [6.80]	— NS*	1.1 (3)	0.6 (3)	1.1 (2) NS*	1.3 (2)
BES	7.18 ± 0.07 (7) [7.17]	— 3.5*	1.7 (2)	1.6 (2)	— NS*	2.5 (2)
HEPES	7.55 ± 0.09 (9) [7.55]	— NS*	NS (2)	1.3 (4)	NS (1) NS*	0.8 (2)
Tricine	8.16 ± 0.04 (8) [8.15]	— 7.3*	5.2 (2)	4.3 (2)	2.3 (2) 2.4*	5.7 (2)

Note that this table gives the metal binding constant,  $K'_M$ , as used for this purpose by Good et al. (1966), which is the inverse of  $K_M$ , as defined in Scheme II. Thus,  $\log K'_M$  is the same as  $pK'_M$ ; i.e., a large number means high affinity binding. The  $pK_a$  values for buffers measured at the same time as metal binding determinations are given as mean ± SD ( $n$ ) to indicate the variability of the measurements. Nominal  $pK_a$  values [ $n$ ] are apparent “practical” values at 20°C and 0.1 M (Perrin and Dempsey, 1974), except that for Homopipes, which was taken from the manufacturer’s literature.  $K'_M$  values were measured at room temperature (20–22°C) and calculated as described in materials and methods from the change in  $pK_a$  of the buffer titrated in the absence or presence of equimolar ZnCl<sub>2</sub> or other metal (Good et al., 1966). Values were calculated from the average shift in  $pK_a$  in ( $n$ ) determinations, thus errors are not given. For NS entries, the measured  $pK_a$  values ± metal were indistinguishable. Values of  $\log K'_M < 1$  are effectively negligible, because  $\log K'_M = 0.7$  if  $\Delta pK_a$  is 0.02 U, a barely detectable difference. \* $K'_M$  values for Ca<sup>2+</sup> and Cu<sup>2+</sup> from Good et al. (1966) are given for comparison. <sup>†</sup>The  $pK_a$  given is  $pK_2$  for titrating the acid, with  $pK_1$  occurring at pH < 3 (Good et al., 1966).

that Table I lists  $\log$  metal dissociation constant ( $K_M$ )<sup>1</sup> values, and that a value <1.3 indicates that >50% of the total metal remains unbound. Thus, much of the binding indicated is rather weak and does not preclude using these buffers in studies of metals.

### Solubility of Zn(OH)<sub>2</sub> and Other Metal Dihydroxides

An upper limit to the concentration of ZnCl<sub>2</sub> is set by the limited solubility of Zn(OH)<sub>2</sub> ( $K_{sp} \approx 4 \times 10^{-17}$ ; Lide, 1995). The maximal soluble concentrations: ~40 μM at pH 8, ~4 mM at pH 7, and ~400 mM at pH 6, were not approached during experiments. We encountered solubility problems when titrating the buffers to test for metal binding (above). For this purpose, we usually used 10 mM ZnCl<sub>2</sub>, and in fact the solutions began to precipitate just above pH 7. To extend the pH range, buffers with higher  $pK_a$  were titrated at 1 instead of 10 mM. The dihydroxide of Cd<sup>2+</sup> is somewhat more soluble ( $K_{sp} 5.27 \times 10^{-15}$ ; Lide, 1995) than that of Zn<sup>2+</sup>, and the maximal attainable concentration is ~5 mM at

pH 8, so solubility was less of a problem. However, when the metal titrations exceeded pH ~8, precipitation commenced.

### Electrophysiology

Conventional whole-cell, cell-attached patch, or inside-out patch configurations were used. Inside-out patches were formed by lifting the pipette into the air briefly. Micropipettes were pulled using a Flaming Brown automatic pipette puller (Sutter Instruments, Co.) from EG-6 glass (Garner Glass Co.), coated with Sylgard 184 (Dow Corning Corp.), and heat polished to a tip resistance ranging typically from 3 to 10 MΩ. Electrical contact with the pipette solution was achieved by a thin sintered Ag-AgCl pellet (In Vivo Metric Systems) attached to a Teflon-encased silver wire. A reference electrode made from a Ag-AgCl pellet was connected to the bath through an agar bridge made with Ringer’s solution. The current signal from the patch clamp (List Electronik) was recorded and analyzed using a Laboratory Data Acquisition and Display System (Indec Corp.). Seals were formed with Ringer’s solution (mM: 160 NaCl, 4.5 KCl, 2 CaCl<sub>2</sub>, 1 MgCl<sub>2</sub>, 5 HEPES, pH 7.4) in the bath, and the zero current potential established after the pipette was in contact with the cell. Bath temperature was controlled by Peltier devices, and monitored by a resistance temperature detector element (Omega Scientific) in the bath.

Because the voltage dependence of H<sup>+</sup> channel gating depends strongly on ΔpH, the threshold for activation ranging from –80 to +80 mV at ΔpH 2.5 and –1.5, respectively (Cherny et al., 1995), the holding potential,  $V_{hold}$ , must be adjusted appropriately.  $V_{hold}$  was set sufficiently negative to the threshold of activation at each ΔpH to avoid Cole-Moore effects (DeCoursey and Cherny, 1994), but positive enough to avoid unnecessarily large voltage steps.

### Conventions

We refer to pH in the format pH<sub>o</sub>/pH<sub>i</sub>. In the inside-out patch configuration, the solution in the pipette sets pH<sub>o</sub>, defined as the pH of the solution bathing the original extracellular surface of the membrane, and the bath solution sets pH<sub>i</sub>. Currents and voltages are presented in the normal sense; that is, upward currents represent current flowing outward through the membrane from the original intracellular surface, and potentials are expressed by defining the original bath solution as 0 mV. Current records are presented without correction for leak current or liquid junction potentials.

### Data Analysis

The time constant of H<sup>+</sup> current activation,  $\tau_{act}$ , was obtained by fitting the current record by eye with a single exponential after a brief delay (DeCoursey and Cherny, 1995) (Eq. 2):

$$I(t) = (I_0 - I_\infty) \exp \frac{-(t - t_{delay})}{\tau_{act}}, \quad (2)$$

where  $I_0$  is the initial amplitude of the current after the voltage step,  $I_\infty$  is the steady state current amplitude,  $t$  is the time after the voltage step, and  $t_{delay}$  is the delay. The H<sup>+</sup> current amplitude is ( $I_0 - I_\infty$ ). No other time-dependent conductances were observed consistently under the ionic conditions employed. Tail current time constants,  $\tau_{tail}$ , were fitted to a single exponential (Eq. 3):

$$I(t) = I_0 \exp \frac{-t}{\tau_{tail}} + I_\infty, \quad (3)$$

where  $I_0$  is the amplitude of the decaying part of the tail current.

<sup>1</sup>Abbreviations used in this paper:  $\alpha$ , cooperativity factor defined in Eq. A6; ΔpH, pH<sub>o</sub> – pH<sub>i</sub>;  $g_{H^+}$ , proton chord conductance; I-V, current-voltage; I<sub>H</sub>, proton current;  $K'_M$ , metal binding constant;  $K_a$ , proton dissociation constant;  $K_M$ , metal dissociation constant.

Data are presented as mean  $\pm$  SD or SEM, as indicated. Significance of differences between groups was calculated by two-tailed student's *t* test.

## RESULTS

*Effects of Extracellular ZnCl<sub>2</sub> on H<sup>+</sup> Currents*

The inhibition of H<sup>+</sup> currents by external ZnCl<sub>2</sub> is illustrated in Fig. 1. The H<sup>+</sup> current elicited by a pulse to +10 mV is reduced in a concentration-dependent manner by ZnCl<sub>2</sub>. The rate the current turns on during a depolarizing voltage pulse is slower, as seen more clearly in Fig. 1 B, where the currents are scaled to the same value at the end of the pulse. Another effect (explored below) is to shift the voltage dependence of H<sup>+</sup> channel gating to more positive voltages. To some extent, the reduced H<sup>+</sup> current amplitude and slower activation can be attributed to this voltage shift. One implication is that any attempt to quantitate the apparent "block" of H<sup>+</sup> currents by ZnCl<sub>2</sub> by measuring the current at the end of a pulse will be arbitrary because the result depends strongly on the length of the pulse and the voltage selected for the measurement. The appar-

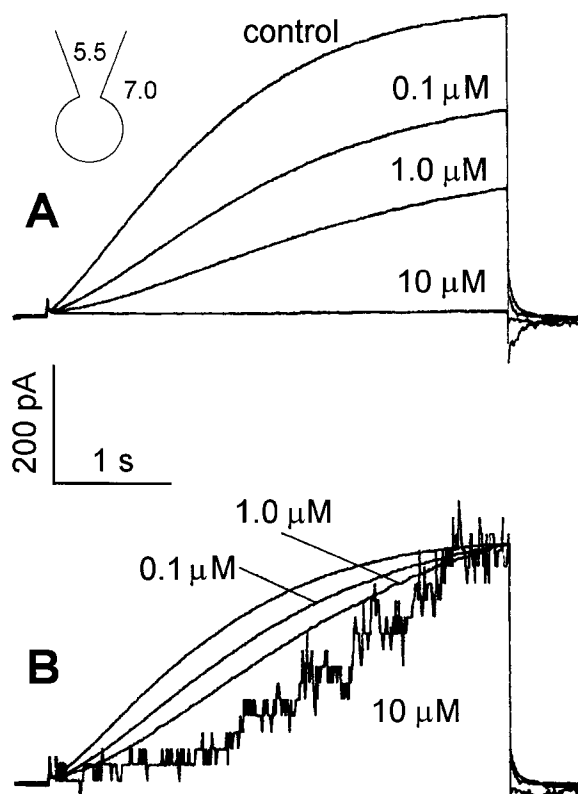


Figure 1. (A) Effects of ZnCl<sub>2</sub> on the H<sup>+</sup> current elicited by a 4-s pulse to +10 mV in a cell studied at pH 7.0//5.5. The inset shows the pH of the pipette and bath solutions. (B) The same currents scaled to the same value at the start and end of the 4-s pulse, illustrating the slowing of the activation time course. The steps in the 10 μM record are due to the resolution of the A-D converter.

ent extent of block at the end of the pulses in Fig. 1 would be greatly reduced if longer test pulses were applied and especially if a more positive test potential were selected.

*Zn<sup>2+</sup> Block Is Not Voltage Dependent*

If ZnCl<sub>2</sub> binds with rapid kinetics to a site in the H<sup>+</sup> channel within the membrane electrical field, this should manifest itself in the instantaneous current-voltage relationship. The control instantaneous current-voltage relationship in Fig. 2 A (●) exhibits

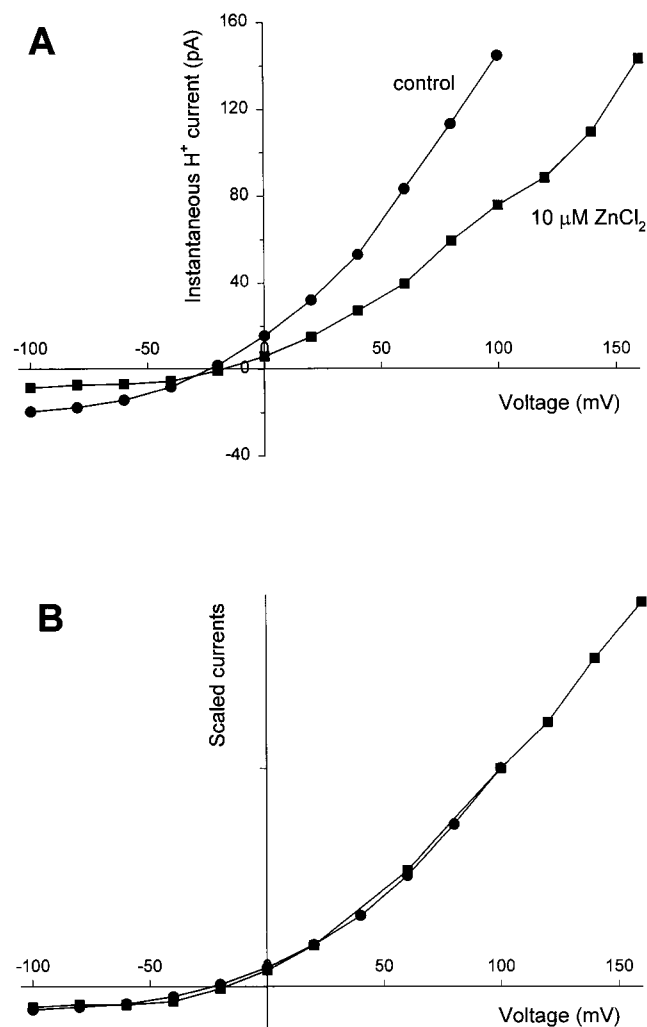
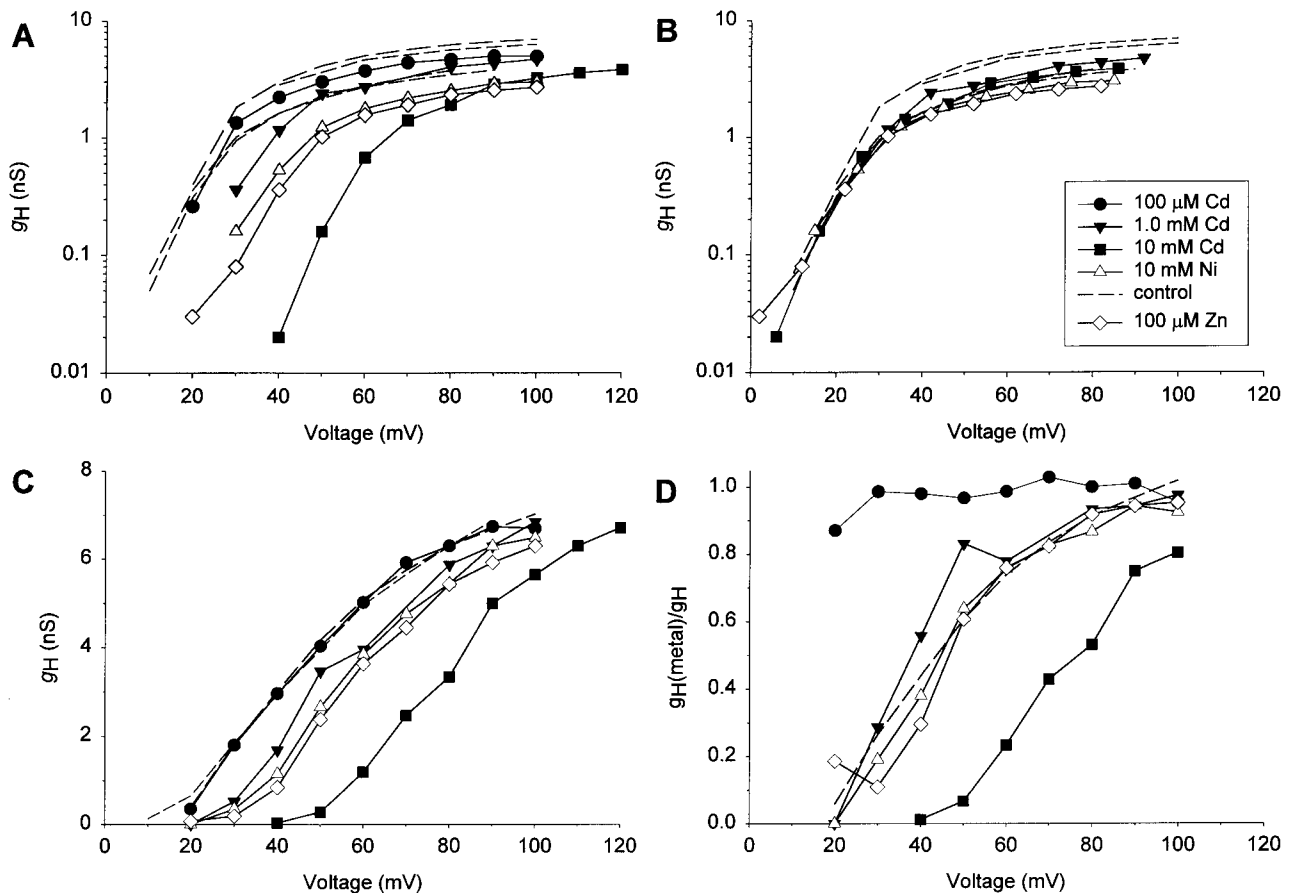


Figure 2. (A) Instantaneous current-voltage relationships in a cell studied at pH 7.0//6.5 before (●) and after (■) addition of 10 μM ZnCl<sub>2</sub> to the bath. A prepulse to +40 mV for control and +100 mV in the presence of ZnCl<sub>2</sub> was applied to open H<sup>+</sup> channels, followed by a test pulse to the voltage on the abscissae. The current at the start of the test pulse, after the capacitive transient, is plotted. (B) Data from A after correction for the current at the end of the prepulse, and normalized to be equal at +100 mV. Dividing the test current by that at the end of the prepulse corrects for variation in the activation of the  $g_{H^+}$  during different prepulses. The symbols have the same meaning as in A.

moderate outward rectification, consistent with previous studies (Byerly et al., 1984; Kapus et al., 1993; Bernheim et al., 1993; Cherny et al., 1995; DeCoursey and Cherny, 1996). The instantaneous I-V relationship in the presence of 10  $\mu\text{M}$   $\text{ZnCl}_2$  (■) is also plotted. The currents are reduced even though the prepulse was 40 mV more positive. After both sets of currents are scaled to match at +100 mV (Fig. 2 B), the currents superimpose, indicating that there is no rapid voltage-dependent block. In some experiments with  $\text{CdCl}_2$ , there was a suggestion that the inward currents were reduced preferentially, but this effect was too small to be sure of, even with data spanning 200 mV. Thus, metals have

negligible effects on the instantaneous I-V relation of  $\text{H}^+$  channels.

The effects of  $\text{ZnCl}_2$  and other metals might reflect voltage-independent interaction of the metal with the channel or nearby membrane. By binding to or screening negative charges near the external side of the  $\text{H}^+$  channel, metals could bias the membrane potential sensed by the channel's voltage sensor (Frankenhaeuser and Hodgkin, 1957). In the simplest scenario, the voltage-dependent properties of the channel will simply shift along the voltage axis. Fig. 3 A illustrates proton chord conductance ( $g_{\text{H}}$ )-V relationships in one cell in the absence (dashed lines) or presence of 100  $\mu\text{M}$



**Figure 3.** Effects of divalent metals on the  $g_{\text{H}}$ -V relationship are incompatible with the idea of voltage-dependent block. (A) The  $g_{\text{H}}$ -V relationships in a cell studied in the presence of several metals: controls (dashed lines), 0.1 mM  $\text{CdCl}_2$  (●), 1 mM  $\text{CdCl}_2$  (▼), 10 mM  $\text{CdCl}_2$  (■), 10 mM  $\text{NiCl}_2$  (△), and 0.1 mM  $\text{ZnCl}_2$  (◇). The sequence was control, all  $\text{CdCl}_2$  concentrations, control,  $\text{NiCl}_2$ ,  $\text{ZnCl}_2$ , and control. (B) The same  $g_{\text{H}}$ -V relationships in A shifted along the voltage axis so that they superimpose at small  $g_{\text{H}}$ . Other than small differences in the limiting  $g_{\text{H,max}}$ , the shape of the voltage dependence appears similar. The voltage shifts applied were: 0, +8, and +34 mV for 0.1, 1.0, and 10 mM  $\text{CdCl}_2$ , respectively, +15 mV for  $\text{NiCl}_2$  and +18 mV for  $\text{ZnCl}_2$ . (C) The same  $g_{\text{H}}$ -V relationships plotted on linear axes and scaled to have similar  $g_{\text{H,max}}$  appear to simply shift along the voltage axis. The scale factor was determined by taking the ratio of  $g_{\text{H}}$  in the presence of metal to that at +80 mV in the first control measurement. To compensate for the apparent voltage shift (compare A and B), the  $g_{\text{H}}$  value used for this purpose for the metal data was shifted by 10 mV (1 mM  $\text{CdCl}_2$ , 10 mM  $\text{NiCl}_2$ ), 20 mV ( $\text{ZnCl}_2$ ), or 30 mV (10 mM  $\text{CdCl}_2$ ). All scale factors were <2.5. (D) The steepness of the apparent voltage dependence of "block" by divalent cations is similar to that of the  $g_{\text{H}}$ -V relationship itself. The data in C are plotted as a ratio of the  $g_{\text{H}}$  in the presence of metal to that in its absence, at each voltage, using the same symbols as other parts of this figure. There is no block at any voltage at 0.1 mM  $\text{CdCl}_2$  (●). The control  $g_{\text{H}}$ -V relationship (C, dashed line) was fitted to a simple Boltzmann distribution and normalized to its fitted maximum. The slope factors of Boltzmann fits were 12.5 mV for control, and for metal ranged from 8 to 13 mV in fits constrained to limit at 1.0.

ZnCl<sub>2</sub> (◇), 10 mM NiCl<sub>2</sub> (△), or several concentrations of CdCl<sub>2</sub> (solid symbols). When shifted along the voltage axis, the  $g_H$ -V relationships appear quite similar (Fig. 3 B), consistent with this mechanism. These metals may reduce the limiting  $g_H$  ( $g_{H,max}$ ) slightly, although for the data shown here this effect was smaller than the variability in the control measurements. At higher metal concentrations, some reduction in  $g_{H,max}$  usually became evident, but was difficult to measure accurately. In Fig. 3 C, the  $g_H$ -V relationships are plotted on linear axes, scaled to the same  $g_{H,max}$  to illustrate their similar shape and slope. The predominant effect is a simple voltage shift.

Even though there is no rapid voltage-dependent block (Fig. 2), the apparent voltage shift might conceivably reflect a slow block/unblock process. If we estimate the steady state voltage dependence of this apparent ZnCl<sub>2</sub> block in the usual manner by plotting the ratio  $I_H(\text{ZnCl}_2)/I_H(\text{control})$ , the apparent block is quite steep. Fig. 3 D shows the ratios for the same experiment as in other parts of this figure. These curves have similar slopes: a simple Boltzmann fit gives slope factors 8–13 mV. However, if the actual effect is a simple voltage shift of the  $g_H$ -V relationship, then the apparent steepness of the “voltage-dependent block” will be identical to the steepness of the Boltzmann relationship in the absence of Zn<sup>2+</sup>. This being the case, the data in Fig. 3 D strongly suggest that metals shift the voltage sensed by the channel rather than binding to the channel in a voltage-dependent manner.

### ZnCl<sub>2</sub> Slows H<sup>+</sup> Channel Opening

A prominent effect of ZnCl<sub>2</sub> is to slow the activation of H<sup>+</sup> currents. We quantified this effect by fitting the turn-on of current during depolarizing pulses to a single exponential, after a delay. This procedure provides a reasonable fit under most conditions. In the presence of ZnCl<sub>2</sub>, both the delay and  $\tau_{act}$  were increased by roughly the same factor. We focussed mainly on metal effects on  $\tau_{act}$ , which are illustrated in Fig. 4 for the same cell shown in Fig. 3. Because the  $\tau_{act}$ -V relationship is nearly exponential (linear on semi-log axes), it is not possible to distinguish whether  $\tau_{act}$  is slowed or its voltage dependence is shifted, or both. In the simplest case of a Huxley-Frankenhaeuser-Hodgkin voltage shift, all kinetic parameters should be shifted equally along the voltage axis. To explore the extent to which this model might apply, the  $\tau_{act}$  data in Fig. 4 B were “corrected” by the voltage shift determined for the  $g_H$ -V relationship (Fig. 3 B). To a rough approximation, the  $\tau_{act}$  effect in CdCl<sub>2</sub> and NiCl<sub>2</sub> appears to be explainable by this simple voltage shift. Closer examination of Fig. 4 B and other data (not shown) at high CdCl<sub>2</sub> concentrations indicates that CdCl<sub>2</sub> slows activation somewhat

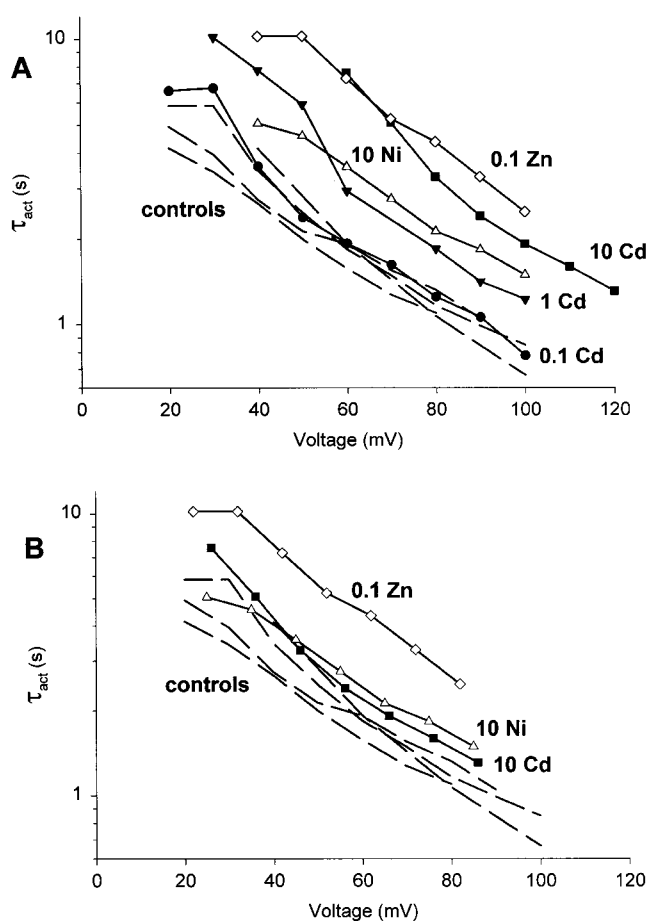


Figure 4. Effects of metals on the activation time constant,  $\tau_{act}$ , in the same cell studied at pH 6.0//5.5 as in Fig. 3. (A) The voltage dependence of  $\tau_{act}$  is plotted in the presence of CdCl<sub>2</sub>, NiCl<sub>2</sub>, and ZnCl<sub>2</sub> at concentrations indicated in the figure (mM). Four control data sets are plotted as dashed lines. The sequence was control twice, CdCl<sub>2</sub>, control, NiCl<sub>2</sub>, ZnCl<sub>2</sub>, and control. (B) The data in the presence of metals is shifted to more negative voltages, according to the shift of the  $g_H$ -V relationship observed in this cell (in Fig. 3). For clarity, only data at 10 mM CdCl<sub>2</sub> (■), 10 mM NiCl<sub>2</sub> (△), and 0.1 mM ZnCl<sub>2</sub> (◇) are plotted. Note that the slowing of  $\tau_{act}$  by CdCl<sub>2</sub> and NiCl<sub>2</sub> appears ascribable to a simple voltage shift, whereas ZnCl<sub>2</sub> has an additional slowing effect.

more than is accounted for by the shift of the  $g_H$ -V relationship, consistent with a previous study of CdCl<sub>2</sub> on H<sup>+</sup> currents (Byerly et al., 1984). In contrast, ZnCl<sub>2</sub> slows channel opening dramatically, and far beyond its shift of the  $g_H$ -V relationship. The effects of ZnCl<sub>2</sub> are dominated by an interaction with the H<sup>+</sup> channel that results in  $\tau_{act}$  slowing, beyond a simple voltage shift of all parameters.

### ZnCl<sub>2</sub> and CdCl<sub>2</sub> Have Minor Effects on H<sup>+</sup> Channel Closing

The tail current decay seemed faster in the presence of external ZnCl<sub>2</sub> or CdCl<sub>2</sub>. However, attempts to evaluate metal effects on H<sup>+</sup> channel closing were hampered by

the tendency of metals to reduce  $H^+$  currents and by the weak voltage dependence of the closing rate (Cherny et al., 1995). The latter property ( $\tau_{tail}$  changes e-fold in  $\sim 50$  mV) means that a 35-mV shift of the  $\tau_{tail}$ -V relationship would change  $\tau_{tail}$  at a given voltage by a factor of only two. Examination of data on  $ZnCl_2$  and  $CdCl_2$  in a number of cells under different conditions gave the impression that the  $\tau_{tail}$ -V relationship may have been shifted in the positive direction at most by roughly the amount that the  $g_H$ -V relationship was shifted, but little effect was seen in some experiments.

#### pH Dependence of Metal Effects

Fig. 5 illustrates the effects of  $ZnCl_2$  on  $H^+$  currents at three  $pH_o$ .  $ZnCl_2$  reduces the  $H^+$  current at each voltage, slows activation, and shifts the voltage dependence

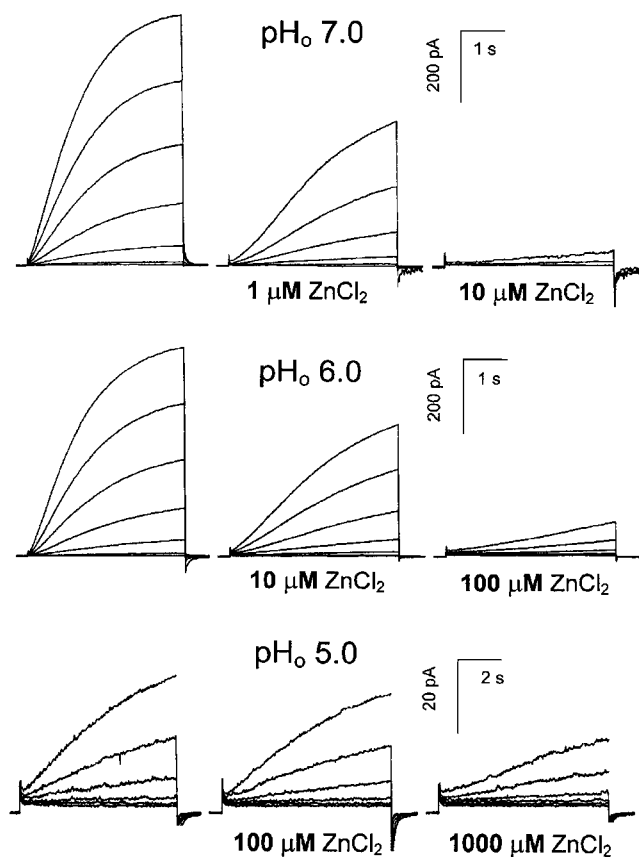


Figure 5. The effects of  $ZnCl_2$  are strongly dependent on  $pH_o$ . Families of voltage-clamp currents are shown at  $pH_o$  7.0, 6.0, and 5.0, with  $pH_i$  5.5, recorded in the absence (left-most family in each row) and presence of the indicated concentration of  $ZnCl_2$ . Data in each row are from the same cell, were recorded during an identical family of voltage pulses, and the same calibration bars apply. The cell at  $pH_o$  7.0 was held at  $-60$  mV, and pulses were applied from  $-40$  to  $+20$  mV in 10-mV increments. The cell at  $pH_o$  6.0 was held at  $-20$  mV and pulses applied from  $+10$  to  $+70$  mV in 10-mV increments. The cell at  $pH_o$  5.0 was held at  $-20$  mV and pulses applied from  $+50$  to  $+100$  mV in 10-mV increments.

of activation to more positive voltages. At each  $pH_o$ , the effects are similar, but the concentration of  $ZnCl_2$  required to produce these effects is much greater at low  $pH_o$ . In this sense, lowering  $pH_o$  decreases the efficacy of  $ZnCl_2$ . To quantitate the effects of  $ZnCl_2$ , we measured  $\tau_{act}$  and calculated the ratio of  $\tau_{act}$  in the presence of  $ZnCl_2$  to that in its absence in the same cell at the same voltage. In most cells, this ratio was the same at all voltages, thus the effect of  $ZnCl_2$  is a uniform voltage-independent slowing. Average ratios at several  $pH_o$  are plotted in Fig. 6 and can be thought of as reflecting the "apparent potency" of  $ZnCl_2$  at various  $pH_o$ . The concentration required to slow  $\tau_{act}$  twofold is ( $\mu M$ ) 0.22 at  $pH_o$  8, 0.46 at  $pH_o$  7, 5.4 at  $pH_o$  6, 89 at  $pH_o$  5.5, and 1,000 at  $pH_o$  5. The apparent potency of  $ZnCl_2$  (estimated for a fourfold slowing of  $\tau_{act}$  where the curves are parallel) decreased only 2.3-fold between  $pH_o$  8 and 7, 10-fold between  $pH_o$  7 and 6, and 103-fold between  $pH_o$  6 and 5.

Most of the buffers used bind  $Zn^{2+}$  detectably (Table I). In Fig. 6 B, the data from Fig. 6 A are replotted after correcting the metal concentrations for binding by buffer. The correction factors are given in the legend. The main effect is to reduce the shift in apparent potency between  $pH_o$  7 and 8. After correction, the concentration required to slow  $\tau_{act}$  twofold is ( $\mu M$ ) 0.22 at  $pH_o$  8, 0.27 at  $pH_o$  7, 4.3 at  $pH_o$  6, 80 at  $pH_o$  5.5, and 1,000 at  $pH_o$  5. The apparent potency of  $ZnCl_2$  (again estimated for a fourfold slowing of  $\tau_{act}$  where the curves are parallel) decreased 1.3-fold between  $pH_o$  8 and 7, 14-fold between  $pH_o$  7 and 6, and 129-fold between  $pH_o$  6 and 5.

Measurements made in the same external solutions with different pipette pH gave no indication that  $pH_i$  affects the interaction between externally applied  $ZnCl_2$  and  $\tau_{act}$ . As illustrated in Fig. 6, there was no obvious difference in the effects of  $ZnCl_2$  at constant  $pH_o$  in cells studied with  $pH_i$  5.5 (solid symbols and continuous lines) or at  $pH_i$  6.5 (open symbols and dashed lines). This result is consistent with externally applied  $ZnCl_2$  exerting its effect at the external side of the membrane.

Besides slowing activation, metals also shift channel opening to more positive voltages. This voltage shift was estimated from graphs of the  $g_H$ -V relationships in the absence or presence of metal and is plotted in Fig. 7. This parameter was somewhat arbitrary and less well defined than  $\tau_{act}$ , because it required extrapolating the fitted time course of  $H^+$  current and measuring  $V_{rev}$  in each solution (whenever  $pH_o$  was changed). Nevertheless, the  $pH_o$  sensitivity of the  $g_H$ -V relationship to  $ZnCl_2$  (solid symbols) qualitatively resembles that of  $\tau_{act}$ . In fact, the interaction between  $ZnCl_2$  and  $pH_o$  manifested in the  $g_H$ -V relationship appears to be somewhat stronger than that for the  $\tau_{act}$ -V relationship. The con-

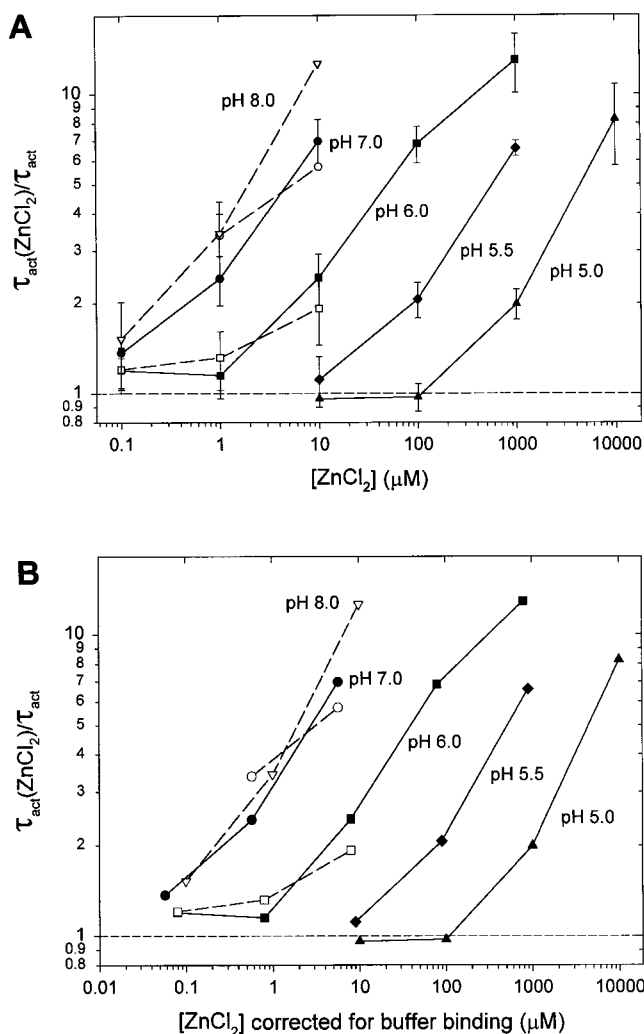


**Figure 6.** (A) Slowing of  $\tau_{act}$  by  $ZnCl_2$  depends strongly on  $pH_o$  ( $\nabla$ ,  $pH_o$  8;  $\bullet$ ,  $\circ$ , 7;  $\blacksquare$ ,  $\square$ , 6.0;  $\blacklozenge$ , 5.5;  $\blacktriangle$ ,  $pH_o$  5) but is independent of  $pH_i$ . Open symbols indicate cells studied at  $pH_i$  6.5, solid symbols at  $pH_i$  5.5. Families of  $H^+$  currents were recorded in the absence and presence of  $ZnCl_2$  in each cell. The  $H^+$  currents were fitted by a single exponential after a delay and the  $\tau_{act}$  data plotted versus voltage, as illustrated in Fig. 4. The ratio of  $\tau_{act}$  in the presence of  $ZnCl_2$  to that in its absence was measured at several voltages and averaged for each cell. When the voltage range did not overlap (as occurred for only a few cells at high  $[ZnCl_2]$ ), the control value was extrapolated from  $\tau_{act}$  data at the highest voltages studied. The mean ratios from three to five different cells at each  $pH_o/pH_i$  are plotted along with SD bars. The dashed line indicates a ratio of 1.0, which means that no effect was observed. (B) The data in A are replotted after correcting for measured metal binding by the buffers used (Table I). The corrections apply to measurements using PIPES and Mes, for which detectable binding of  $ZnCl_2$  was measured. The calculated correction factors that give the fraction of total applied  $[ZnCl_2]$  that is unbound by buffer are: 0.576 for  $pH_o$  7.0, 0.798 for  $pH_o$  6.0, and 0.90 for  $pH_o$  5.5, calculated from  $[M]_{free}/[M]_{total} = 1/(1 + K'_M[B^-])$ , where the deprotonated buffer concentration  $[B^-]$  was calculated by the Henderson-Hasselbalch equation according to the buffer  $pK_a$  and pH. No correction was applied at  $pH_o$  8.0 or 5.0 because no binding of  $ZnCl_2$  to HEPES or Homopipes, respectively, was detected (Table I).

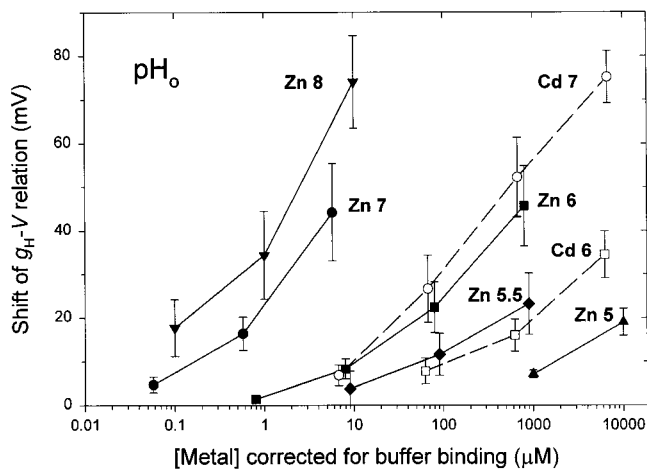
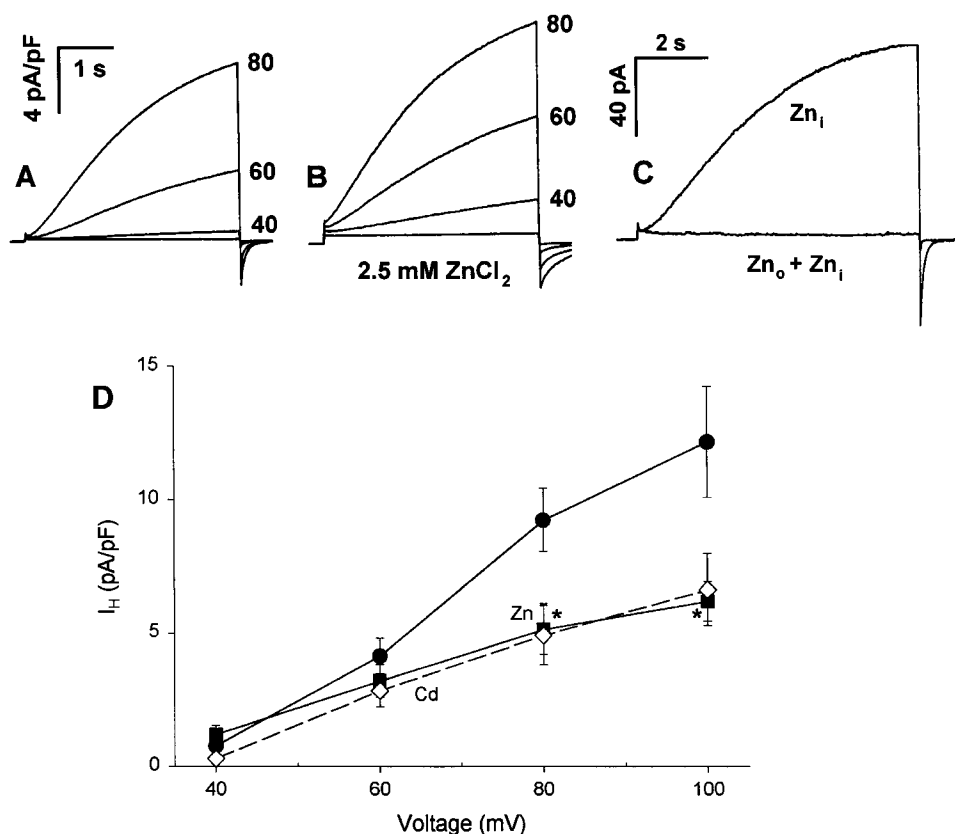


**Figure 7.** The shift in the voltage dependence of activation of the  $g_H$  produced by  $ZnCl_2$  or  $CdCl_2$  depends strongly on  $pH_o$ . Mean shift  $\pm$  SD are plotted for two to seven determinations in each condition (91 total). Filled symbols connected by solid lines represent  $ZnCl_2$  and open symbols with dashed lines indicate  $CdCl_2$  measurements, and the numbers indicate  $pH_o$ . The shift was estimated by plotting  $g_H$ -V relationships and measuring the apparent voltage shift for comparable levels of  $g_H$ . The estimate was made arbitrarily when  $g_H$  was large enough to be reliably determined, but always at  $<50\%$  of  $g_{H,max}$  because any reduction in  $g_{H,max}$  (which might have a different mechanism) would contaminate the measurement.  $ZnCl_2$  and  $CdCl_2$  concentrations have been corrected for buffer binding as described in Fig. 6. The calculated unbound fraction of  $CdCl_2$  was 0.672 at  $pH_o$  7 and 0.626 at  $pH_o$  6. Because  $pH_i$  had no detectable effect on externally applied metals (Fig. 6), we combined results here for  $pH_i$  5.5 and 6.5. For all data at  $pH_o$  8.0,  $pH_i$  was 6.5, measurements at  $pH_o$  7 and 6 include both  $pH_i$  5.5 and 6.5, and for all data at  $pH_o$  5.5 or 5.0,  $pH_i$  was 5.5.

concentration of  $ZnCl_2$  required to produce a 20-mV depolarizing shift of the  $g_H$ -V relationship was 0.13  $\mu M$  at  $pH_o$  8.0, 0.77  $\mu M$  at  $pH_o$  7.0, 54  $\mu M$  at  $pH_o$  6.0, 470  $\mu M$  at  $pH_o$  5.5, and 12.4 mM (by extrapolation) at  $pH_o$  5.0. The apparent potency of  $ZnCl_2$  thus decreased sixfold between  $pH_o$  8 and 7, 70-fold between  $pH_o$  7 and 6, and 230-fold between  $pH_o$  6 and 5. The larger difference between the effective potency of  $ZnCl_2$  between  $pH_o$  7 and  $pH_o$  8 requires a higher  $pK_a$  for the steady state conductance measurement than for the kinetic  $\tau_{act}$  measurement (see discussion).

#### Effects of Intracellular $ZnCl_2$ on $H^+$ Currents

Effects of internally applied  $ZnCl_2$  were studied in the whole-cell configuration and in inside-out patches. Fig. 8 illustrates families of  $H^+$  currents in cells studied at  $pH$  6.5//6.5 without (A) and with (B) 2.5 mM  $ZnCl_2$  added to the pipette solution. The  $H^+$  currents appear generally similar, although closer inspection reveals that the tail currents decayed more slowly in the cell with internal  $ZnCl_2$ . The pipette solution contained 1 mM EGTA and BisTris buffer (which will bind  $\sim 90\%$  of the  $Zn^{2+}$  under these conditions, Table I), so the addi-



control cells (●), 9–14 cells studied with 2.5 mM ZnCl<sub>2</sub> added to the pipette solution (■), and 3 cells studied with 2.5 mM CdCl<sub>2</sub> in the pipette solution (◇), all at pH 6.5//6.5. \*Values for ZnCl<sub>2</sub> at +80 and +100 mV differ significantly from control ( $P < 0.05$ ).

tion of 2.5 mM ZnCl<sub>2</sub> results in a free [Zn<sup>2+</sup>] ~170 μM. Fig. 8 C illustrates that addition of the pH 6.5 ZnCl<sub>2</sub> containing pipette solution to the bath dramatically reduced the H<sup>+</sup> current at +50 mV. This result makes it clear that ZnCl<sub>2</sub> applied externally is much more effective than when applied internally. Several cells were studied with 2.5 mM ZnCl<sub>2</sub> in the pipette at pH<sub>i</sub> 7.5. HEPES buffer does not bind ZnCl<sub>2</sub> detectably (Table I), hence the free [ZnCl<sub>2</sub>] was ~1.5 mM. In these cells, the H<sup>+</sup> currents also appeared normal (data not shown).

Our impression was that there was nothing unusual in the behavior of the  $g_H$  in these experiments. H<sup>+</sup> currents were studied after allowing at least 5–10 min equilibration of the ZnCl<sub>2</sub>-containing pipette solution. The amplitude of  $I_H$  did not change consistently during the experiment. The mean  $I_H$  normalized to the input capacity (Fig. 8 D) was reduced significantly ( $P < 0.05$ ) at +80 and +100 mV in cells studied with 2.5 mM ZnCl<sub>2</sub> in the pipette, on average after 29 min in whole-cell configuration. Internal ZnCl<sub>2</sub> at high concentrations reduces  $I_H$ , but this effect is not very pronounced.

Fig. 9 illustrates mean  $\tau_{act}$  values in cells studied at pH 6.5//6.5 with (■) and without (□) 2.5 mM ZnCl<sub>2</sub> in the pipette solution. No difference in the kinetics of H<sup>+</sup> current activation was detected. However, channel

closing was significantly slower in cells studied with internal ZnCl<sub>2</sub>. Fig. 9 shows mean values of  $\tau_{tail}$  in cells studied with internal ZnCl<sub>2</sub> (●) and in control cells (○). The deactivation rate on average was 3.1-fold slower with internal ZnCl<sub>2</sub> (measured between –50 and +10 mV). In three cells studied with 2.5 mM CdCl<sub>2</sub> added to the pipette solutions, the average slowing of  $\tau_{tail}$  was 1.8-fold at 10 voltages from –80 to +20 mV ( $P < 0.05$  at each voltage) (not shown). Applied internally, ZnCl<sub>2</sub> thus slows closing without affecting activation. In contrast, externally applied ZnCl<sub>2</sub> slowed activation and, if anything, accelerated deactivation. Clearly the internal and external sites of action of ZnCl<sub>2</sub> are functionally quite different.

A concern during these experiments was the extent to which ZnCl<sub>2</sub> in the pipette solution actually diffused into the cell. ZnCl<sub>2</sub> diffusion into the cell will be slowed by binding to cytoplasmic proteins, acting as fixed buffers. That measurable effects on  $\tau_{tail}$  were seen is evidence that the ZnCl<sub>2</sub> diffused into the cells to a significant extent. The mobility of ZnCl<sub>2</sub> is not unusually small (Robinson and Stokes, 1959).  $V_{rev}$  values were consistent with the applied  $\Delta pH$  (pH 6.5//6.5, Nernst potential = 0 mV), suggesting that buffer from the pipette solution diffused into the cell. In 11 cells studied

Figure 8. High concentrations of intracellular ZnCl<sub>2</sub> have only subtle effects on H<sup>+</sup> currents. The families of H<sup>+</sup> currents at pH 6.5//6.5 were recorded in a control cell (A) and with 2.5 mM ZnCl<sub>2</sub> in the pipette solution (B), and are scaled according to membrane capacity. The measured  $V_{rev}$  was +4 mV in A and +1 mV in B. Note the slower tail current decay with ZnCl<sub>2</sub> in the pipette. Considering binding of ZnCl<sub>2</sub> to 1 mM EGTA and 100 mM BisTris in the pipette solution, the free [Zn<sup>2+</sup>] was ~170 μM. (C) Identical 8-s pulses to +50 mV were applied before and after addition of the pipette solution used in B to the bath, in the same cell shown in A, demonstrating the dramatic effects of this solution applied externally. The threshold for activating outward H<sup>+</sup> current shifted from +30 to +60 mV after adding ZnCl<sub>2</sub> to the bath (determined using high gain and 5-mV increments). (D) Average (mean ± SEM) H<sup>+</sup> current–voltage relationships normalized according to membrane capacity, in 6–10

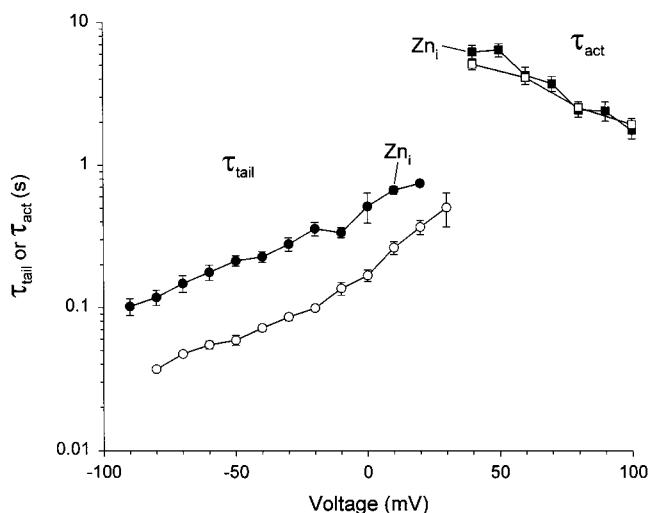


Figure 9. Effects of intracellular  $\text{ZnCl}_2$  on the mean ( $\pm$ SEM) activation time constant,  $\tau_{\text{act}}$ , and deactivation time constant,  $\tau_{\text{tail}}$ , in cells studied at pH 6.5//6.5. Tail current decay was fitted with a single exponential in three to nine control cells ( $\circ$ ) and in four to eight cells studied with 2.5 mM  $\text{ZnCl}_2$  added to the pipette solution ( $\bullet$ ). All  $\tau_{\text{tail}}$  values with  $\text{ZnCl}_2$  in the pipette differ significantly from control ( $P < 0.01$ ). Values of  $\tau_{\text{act}}$  obtained by fitting a single exponential after a delay are plotted from 10–12 control cells ( $\square$ ) and from four to nine cells studied with 2.5 mM  $\text{ZnCl}_2$  added to the pipette solution ( $\blacksquare$ ).

with 2.5 mM  $\text{ZnCl}_2$  in the pipette,  $V_{\text{rev}}$  averaged  $-1.3 \pm 2.4$  mV (mean  $\pm$  SEM). To confirm that  $\text{ZnCl}_2$  entered the cell, we used TPEN, a membrane-permeant metal chelator with a high affinity for  $\text{Zn}^{2+}$  (Arslan et al., 1985). Shortly after addition of 250  $\mu\text{M}$  TPEN to cells studied with  $\text{ZnCl}_2$ -containing pipette solutions, the tail current kinetics became more rapid. On average, the ratio of  $\tau_{\text{tail}}$  before/after TPEN was  $1.65 \pm 0.32$  (mean  $\pm$  SD,  $n = 7$ ), measured at pH 6.5//6.5 at  $-20$  or  $-40$  mV. This is in qualitative agreement with the threefold slowing of  $\tau_{\text{tail}}$  observed in the groups of cells studied with or without internal  $\text{ZnCl}_2$  (Fig. 9). Addition of TPEN to three cells studied with metal-free pipette solutions did not affect  $\tau_{\text{tail}}$  detectably.

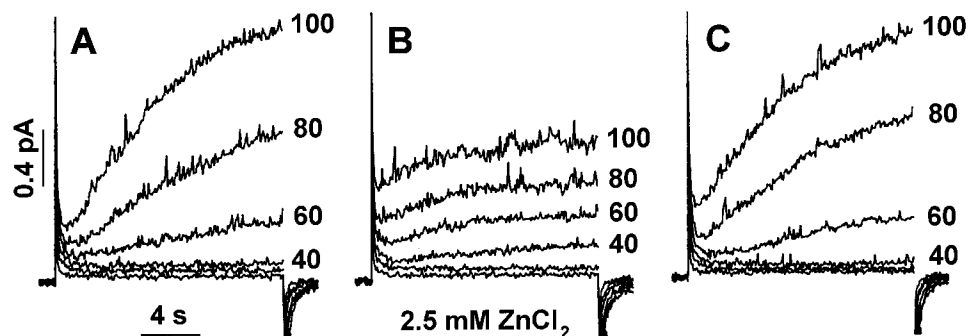


Figure 10. Effects of intracellular  $\text{ZnCl}_2$  on  $\text{H}^+$  currents in an inside-out patch studied at pH 6.5//6.5. The first family (A) was recorded within 5 min after forming the inside-out patch. The family in B was recorded starting 2.5 min after addition of 2.5 mM  $\text{ZnCl}_2$ , and the family in C was recorded starting 1.5 min after washout. In all parts, the cell was held at  $-40$  mV, and 16-s pulses were applied in 20-mV increments. Calibration bars in A apply to all families.

### Measurements in Excised Patches

Inside-out patches were studied at pH<sub>o</sub> 7.5 or 6.5 (pipette pH) and pH<sub>i</sub> 6.5 (bath pH). Addition of 2.5 mM  $\text{ZnCl}_2$  to the bath ( $\sim 170$   $\mu\text{M}$  free  $\text{Zn}^{2+}$ ) reduced the  $\text{H}^+$  current amplitude (Fig. 10 B). This effect of  $\text{ZnCl}_2$  was reversible upon washout (Fig. 10 C). The reduction of  $\text{H}^+$  currents was similar to that observed in whole-cells dialyzed with  $\text{ZnCl}_2$  containing pipette solutions (Fig. 8 D), suggesting that similar concentrations were reached in the whole-cell experiments. There was no clear shift of the voltage dependence of gating. If anything, there was sometimes a small shift to more negative voltages. A small hyperpolarizing shift might be explainable by the slight lowering of pH after addition of  $\text{ZnCl}_2$  to the solution (0.023 U calculated, 0.05 U measured), due to displacement of protons from buffer. In some inside-out patches, the  $\text{H}^+$  currents decreased progressively and gradually after addition of  $\text{ZnCl}_2$ . Spontaneous rundown may account for this largely irreversible loss of  $\text{H}^+$  current. In summary, the inside-out patch data support the conclusion that effects of internally applied  $\text{ZnCl}_2$  differ qualitatively as well as quantitatively from those of externally applied  $\text{ZnCl}_2$ . Internal application of high concentrations of  $\text{ZnCl}_2$  produces only modest effects.

### Effects of $\text{CdCl}_2$ on $\text{H}^+$ Currents

Although we intended to study  $\text{ZnCl}_2$  as a prototype for the effects of all polyvalent cations on  $\text{H}^+$  currents, there were subtle differences between the effects of  $\text{ZnCl}_2$  and  $\text{CdCl}_2$ . Both metals slowed activation and shifted the  $g_{\text{H}}\text{-V}$  relationship to more positive voltages. However, to a first approximation, the effects of  $\text{CdCl}_2$  could be viewed as a simple shift of all parameters to more positive voltages. “Correction” of the  $\tau_{\text{act}}\text{-V}$  relationships in Fig. 4 according to the shift observed in the  $g_{\text{H}}\text{-V}$  relationship in Fig. 3 normalized the data for  $\text{CdCl}_2$ , but not for  $\text{ZnCl}_2$ . In other words,  $\text{ZnCl}_2$  has a pronounced additional slowing effect. Examination of  $\tau_{\text{act}}$  data in individual cells revealed that  $\text{ZnCl}_2$  effects

could usually be approximated as uniform slowing at all voltages, whereas the relative slowing by  $\text{CdCl}_2$  sometimes decreased for larger depolarizations. As a result of this subtle difference, there was not a unique “slowing factor” for  $\text{CdCl}_2$ , and we did not try to plot  $\text{CdCl}_2$  data in Fig. 6. The slowing of  $\tau_{\text{act}}$  by  $\text{CdCl}_2$  was strongly  $\text{pH}_o$  dependent, however. To a first approximation, the  $\text{pH}_o$  dependence of  $\text{CdCl}_2$  was similar to that of  $\text{ZnCl}_2$ .

Another difference between metals is evident in Fig. 7. The shifts of the  $g_{\text{H}}-V$  relationships indicate that  $\text{CdCl}_2$  is  $\sim 30\times$  less potent at either  $\text{pH}_o$  7 or 6. In contrast, the slowing of  $\tau_{\text{act}}$  by  $100 \mu\text{M}$   $\text{ZnCl}_2$  exceeded that by  $10 \text{ mM}$   $\text{CdCl}_2$  over most voltages (Fig. 4 A), and thus there is a  $>100$ -fold difference in potency for this effect. Thus the relative potency of the two metals for slowing  $\tau_{\text{act}}$  and shifting the  $g_{\text{H}}-V$  relationship differs. Perhaps distinct binding sites are involved in these effects, and the relative affinities of the metals for the sites differ.  $\text{ZnCl}_2$  has a high affinity for the site that slows activation, whereas most of the effects of  $\text{CdCl}_2$  are consistent with binding to a “nonspecific” site that shifts the apparent membrane potential sensed by the  $\text{H}^+$  channel.

## DISCUSSION

Polyvalent cations and protons have similar effects on many ion channels (Hille, 1968; Woodhull, 1973; Kwan and Kass, 1993; Arkett et al., 1994), perhaps because they bind to similar sites. It has been postulated that the function of voltage-gated proton channels requires at least two distinct types of protonation sites. Conduction likely occurs via a hydrogen-bonded chain (Nagle and Morowitz, 1978; DeCoursey and Cherny, 1994, 1995, 1997, 1998, 1999a,b), in which case the entryway of the “channel” is a protonation site, where  $\text{H}^+$  must bind to initiate permeation. The second type of protonation sites are allosteric regulatory sites (Byerly et al., 1984) that govern the strong  $\Delta\text{pH}$  ( $\Delta\text{pH} = \text{pH}$  gradient  $= \text{pH}_o - \text{pH}_i$ ) dependence of gating; i.e., the  $40 \text{ mV}/U$  shift in the voltage-activation curve with changes in either  $\text{pH}_o$  or  $\text{pH}_i$  (Cherny et al., 1995). The  $\Delta\text{pH}$ -dependent gating mechanism was explained economically by assuming identical internally and externally accessible regulatory protonation sites (Cherny et al., 1995). More recent evidence suggests the internal and external sites have distinct chemical properties (DeCoursey and Cherny, 1997).

Given this background,  $\text{H}^+$  channels might be affected by  $\text{Zn}^{2+}$  in several ways. (a) Binding at or near the entry to the channel should inhibit  $\text{H}^+$  current by preventing  $\text{H}^+$  binding or reducing the local  $[\text{H}^+]$  available to enter the channel. The attenuation of  $g_{\text{H,max}}$  at high metal concentrations might reflect local  $\text{H}^+$  depletion by this mechanism. However, most of the effects of metals are not compatible with metal binding

to and occluding the channel entry. (b) Binding to a site remote from the entry but which is sensed by the voltage sensor of the channel could shift the position of the voltage dependency of gating, the most simple mechanism of which would result in all voltage-dependent parameters shifting equally along the voltage axis. This mechanism is consistent with most of the effects of  $\text{Cd}^{2+}$  and  $\text{Ni}^{2+}$ . (c) Binding near the allosteric sites on either side of the membrane might reduce the local  $[\text{H}^+]$  electrostatically, and hence affect gating in the same manner as an increase in pH. The effects of metals are in the wrong direction for this mechanism to apply. (d) Finally, metal binding to the allosteric protonation sites might have a similar effect on gating as protonation of these sites, and might thus mimic the effects of low pH near the site. The details of the effects in this case are hard to predict, because due to differences in binding kinetics and steric factors,  $\text{Zn}^{2+}$  can hardly be expected to mimic a single  $\text{H}^+$ , or even two  $\text{H}^+$ . Nevertheless, most of the effects of  $\text{Zn}^{2+}$  can be explained by assuming that it binds to the same regulatory sites as protons, and has the same effects as protons in our model (Cherny et al., 1995). Thus,  $\text{Zn}^{2+}$  (or  $\text{H}^+$ ) binding at the external site prevents channel opening, and  $\text{Zn}^{2+}$  (or  $\text{H}^+$ ) binding at the internal site prevents channel closing.

### *$\text{Zn}^{2+}$ Is Not a Voltage-dependent Blocker of $\text{H}^+$ Channels*

Although polyvalent cation effects on  $\text{H}^+$  currents in various cells are quite similar, some authors have characterized these effects as modification of the voltage dependence of gating (Byerly et al., 1984; Barish and Baud, 1984; DeCoursey, 1991; Kapus et al., 1993; DeCoursey and Cherny, 1993, 1994; 1996; Demaurex et al., 1993), whereas others describe the effects as voltage-dependent block (Bernheim et al., 1993; Gordienko et al., 1996). These views are not equivalent. The voltage dependence of ionic block is generally assumed to arise from the entry of the blocker into the channel pore partway across the membrane potential field, where it gets stuck, physically occluding the pore. Interpreted in terms of voltage-dependent block, metal binding affinity depends strongly on voltage (Bernheim et al., 1993; Gordienko et al., 1996), whereas effects due to binding to a modulatory site can be explained with a fixed  $K_{\text{M}}$ . Because the instantaneous I-V relation was simply scaled down by  $\text{ZnCl}_2$  with no detectable voltage dependence (Fig. 2), we ruled out the possibility of rapidly reversible binding of  $\text{Zn}^{2+}$  to a site within the membrane potential field.

Even though there is no rapidly reversible block, the more obvious effects of  $\text{ZnCl}_2$  could be due to a slow time-dependent block/unblock. Five arguments oppose the idea that the slow activation of  $\text{H}^+$  current in the presence of  $\text{Zn}^{2+}$  reflects voltage-dependent un-

binding of  $\text{Zn}^{2+}$  from the channel. (a) If  $\tau_{\text{act}}$  in the presence of metals (several seconds) reflects the unblock rate, then block must have very slow kinetics. If we assume that  $pK_M = 6.5$  (Fig. 11) and that the binding rate of  $\text{Zn}^{2+}$  is  $3 \times 10^7 \text{ M}^{-1} \text{ s}^{-1}$ , a characteristic rate of complex formation between  $\text{Zn}^{2+}$  and proteins (Eigen and Hammes, 1963), then the unbinding rate is  $9.5 \text{ s}^{-1}$ . Thus,  $\text{Zn}^{2+}$  probably binds and unbinds in a fraction of a second. If the kinetics are rapid, effects should have been manifested in the instantaneous I-V relation. (b) In normal drug-receptor reactions, the unblock rate is independent of concentration. However, increasing the concentration of  $\text{ZnCl}_2$  slowed  $\text{H}^+$  current activation progressively. There was no indication that two populations of gating behavior resulted, as would be predicted if  $\text{ZnCl}_2$  modified a fraction of channels that then opened slowly, with the remaining channels opening at the normal rate. A single exponential (after a delay) continued to fit the data at all  $[\text{ZnCl}_2]$ . Thus it appears that  $\text{ZnCl}_2$  binds and unbinds the channel repeatedly during a single pulse, with the slowing effect related to the fraction of time  $\text{ZnCl}_2$  is bound to the channel. (c) The steady state voltage dependence of this apparent  $\text{Zn}^{2+}$  block, defined as the ratio  $I_{\text{H}}(\text{Zn}^{2+})/I_{\text{H}}(\text{control})$ , is quite steep: a simple Boltzmann fit gives slope factors 8–13 mV (Fig. 3 D). In terms of traditional voltage-dependent block mechanisms (Woodhull, 1973), if  $z$  is the charge on the blocking ion and  $\delta$  is the fraction of the membrane potential sensed by the ion at the block site, then  $z\delta \geq 2.0$ , which implies that  $\text{Zn}^{2+}$ ,  $\text{Cd}^{2+}$ , and  $\text{Ni}^{2+}$  traverse  $\geq 100\%$  of the membrane field to reach the block site. Several examples of  $\delta > 1.0$  for ionic blockade exist in the  $\text{K}^+$  channel literature and are traditionally explained by interaction between permeant ions in a multiply occupied channel (e.g., Hille and Schwarz, 1978). Because it is unlikely for a hydrogen-bonded-chain conduction mechanism to support multiple protons simultaneously, especially at physiological pH (DeCoursey and Cherny, 1999a), explaining the high  $z\delta$  observed for divalent cation “blockade” is problematic. (d) If  $\text{ZnCl}_2$  simply shifted the  $g_{\text{H}}-V$  relationship along the voltage axis, then the apparent steepness of the block, defined as the ratio  $I_{\text{H}}(\text{Zn}^{2+})/I_{\text{H}}(\text{control})$ , will be precisely identical to the steepness of the  $g_{\text{H}}-V$  relationship in the absence of  $\text{Zn}^{2+}$ . The slopes of the fractional block curves, 8–13 mV (Fig. 3D), and control  $g_{\text{H}}-V$  relationships, 8–10 mV (DeCoursey and Cherny, 1994; Cherny et al., 1995), are the same, consistent with a simple voltage shift. (e) Finally, any part of the  $\text{H}^+$  channel conductance pathway comprised of hydrogen-bonded chain would not allow  $\text{Zn}^{2+}$  passage; thus the possibility for voltage-dependent block by  $\text{Zn}^{2+}$  could exist only in an aqueous vestibule. We conclude that polyvalent cations do not exert their effects by entering into the pore, but instead bind to sites on the channel

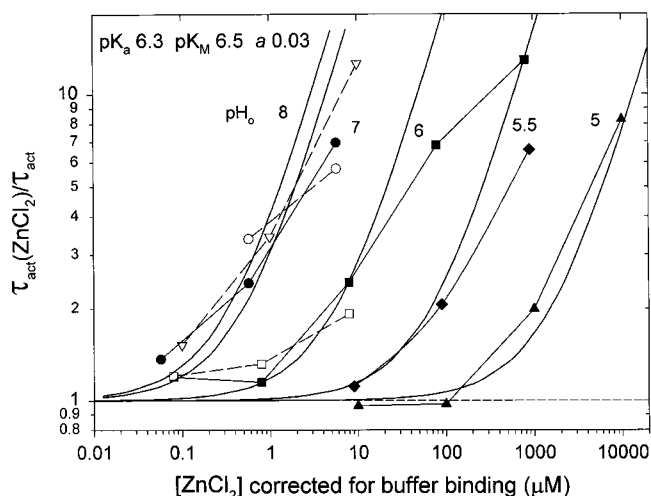


Figure 11. Comparison of the  $\tau_{\text{act}}$  data replotted from Fig. 6 with the slowing predicted by Eq. A6, assuming that the  $\text{H}^+$  channel cannot open while  $\text{Zn}^{2+}$  is bound to its receptor (see text for details). The meaning of the symbols is the same as in Fig. 6, and all curves are the predictions for  $pK_a$  6.3,  $pK_M$  6.5, and cooperativity factor  $a = 0.03$ .

that are accessible to the solution and outside of the membrane potential field. Binding must be specific because different divalent cations have very different concentration dependencies. For example, effects of micromolar concentrations of  $\text{Zn}^{2+}$  are seen in the presence of millimolar  $[\text{Ca}^{2+}]_o$  or  $[\text{Mg}^{2+}]_o$ .

Byerly et al. (1984) proposed that divalent cations bind specifically to a site on the external side of  $\text{H}^+$  channels, based on their observation that the  $g_{\text{H}}-V$  relationship was shifted less by  $\text{CdCl}_2$  than was the  $\tau_{\text{act}}-V$  (actually  $t_{1/2}-V$ ) relationship. For epithelial  $\text{H}^+$  channels, the disparity in effects on channel opening compared with the  $g_{\text{H}}-V$  relationship was even more pronounced for  $\text{ZnCl}_2$  than for  $\text{CdCl}_2$ . A similar sequence of voltage shifts by  $\text{ZnCl}_2$  ( $\tau_{\text{act}}-V > g_{\text{H}}-V > \tau_{\text{tail}}-V$ ) was seen for  $\text{K}^+$  channels (Gilly and Armstrong, 1982). Their interpretation was that  $\text{Zn}^{2+}$  binds to a site on the external side of the channel that is exposed to the bath solution only when the channel is closed. This is precisely the nature of the proposed external modulatory protonation site in our model of  $\text{H}^+$  channel gating (Cherny et al., 1995). The site must be deprotonated before the channel can open, and during the opening process the site “disappears” and the same site (or a distinct site) appears on the internal side of the membrane. It was necessary to assume that the protonation sites were not accessible to both sides of the membrane at the same time to account for the  $\Delta\text{pH}$  dependence of gating.

#### *Zn<sup>2+</sup> Is the Active Species of Zinc*

In solution, zinc exists as several chemical species, whose relative proportions depend strongly on pH.

One plausible explanation for the increased apparent potency of  $\text{ZnCl}_2$  at higher pH is that  $\text{ZnOH}^+$ , rather than the divalent form, is the species acting on  $\text{H}^+$  channels. As pH is increased, the proportion of  $\text{ZnCl}_2$  in monohydroxide form,  $\text{ZnOH}^+$ , increases 10-fold/U, up to  $\sim\text{pH } 8$  (Baes and Mesmer, 1976). The absolute concentration of  $\text{ZnOH}^+$  is a small fraction of the total, and  $>90\%$  of  $\text{ZnCl}_2$  is divalent at  $\text{pH} < 8.0$ , hence  $[\text{Zn}^{2+}]$  remains relatively constant (Baes and Mesmer, 1976). Spalding et al. (1990) concluded that  $\text{ZnOH}^+$  was the active form for  $\text{Cl}^-$  currents in muscle. The "consensus" potency sequence for inhibiting  $\text{H}^+$  currents by divalent metal cations,  $\text{Cu} < \text{Zn} > \text{Ni} > \text{Cd} > \text{Co} > \text{Mn} > \text{Ba}, \text{Ca}, \text{Mg} < 0$  (DeCoursey, 1998), is intriguingly similar to the tendency of these cations to hydrolyze (Perrin and Dempsey, 1974) (indicated by their  $pK_a$ ):  $\text{Cu} (8.0) > \text{Co} (8.9), \text{Zn} (9.0) > \text{Ni}, \text{Cd} (9.9) > \text{Mn} (10.6) > \text{Mg} (11.4) > \text{Ca} (12.6) > \text{Ba} (13.4)$ .

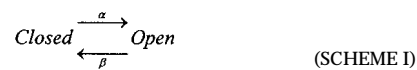
The  $pK_a$  sequence generally reveals the proportion of total metal in monohydroxide form at a given pH. If the monohydroxide form were active, then the apparent potency for all of these metals should increase  $\sim 10$ -fold per unit increase in pH, and the pH dependence should saturate around the  $pK_a$ . We show here that the apparent potency of both  $\text{ZnCl}_2$  and  $\text{CdCl}_2$  increase at higher pH, and the  $\text{pH}_0$  dependence saturates for  $\text{ZnCl}_2$ . However, saturation occurs at a pH that is too low by  $\sim 1$  U, and the change at low  $\text{pH}_0$  is at least 100-fold/U (Figs. 5–7), both inconsistent with the hypothesis that the monohydroxide form is active. If  $\text{ZnOH}^+$  were the active form, an additional mechanism (e.g., competition with  $\text{H}^+$ ) would be required to enhance the pH sensitivity of its effects. Several polyhydroxide forms of zinc (with net negative charge) also are increasingly represented at high pH, but we rule these out as candidates for interaction with the  $\text{H}^+$  channel because (a) it seems unlikely that anions and protons would compete for the same sites, and (b) the fraction of all of these forms combined at  $\text{pH } 5$  is  $< 10^{-12}$  of the total  $\text{ZnCl}_2$  present (Baes and Mesmer, 1976). In conclusion, the most probable form of  $\text{ZnCl}_2$  active on  $\text{H}^+$  channels is the divalent form.

#### *Model of the Interaction between $\text{Zn}^{2+}$ and $\text{H}^+$ that Slows Activation*

The appendix explores the predictions of several possible mechanisms of competition between  $\text{Zn}^{2+}$  and  $\text{H}^+$  for hypothetical binding sites on  $\text{H}^+$  channels. The  $\text{pH}_0$  dependence of  $\text{Zn}^{2+}$  effects on  $\tau_{\text{act}}$  are reasonably compatible with Models 4, 5, or 6 (see Fig. 13 for all models). These models assume that the external  $\text{Zn}^{2+}$  receptor on proton channels is formed by multiple protonation sites that are accessible to the external solution and that coordinate the binding of a single  $\text{Zn}^{2+}$ . If  $\text{H}^+$

and  $\text{Zn}^{2+}$  compete directly for the same site(s), then at least two to three protonation sites must exist. If  $\text{H}^+$  and  $\text{Zn}^{2+}$  bind to different sites, then there must be substantial interaction between them, and the range of the pH dependence indicates that protonation of one site lowers the affinity of the remaining site(s) for  $\text{Zn}^{2+}$  by a factor  $\sim 30$ . Similar binding constants reproduce the pH dependence of  $\text{Zn}^{2+}$  effects using any of several models:  $pK_M$  is 6.5 and  $pK_a$  is 6.2–6.6 and is somewhat model dependent.

To apply the model equations in the appendix to real data, it is necessary to define the effect that metal binding has on channel behavior. By making one assumption, we can define the entire body of  $\tau_{\text{act}}$  data in Fig. 6. We assume that when  $\text{Zn}^{2+}$  is bound to its receptor on the  $\text{H}^+$  channel, the channel cannot open. For the simplest case of a two-state channel, with Scheme I:



where  $\alpha$  is the opening rate and  $\beta$  is the closing rate, the time constant is  $(\alpha + \beta)^{-1}$ . Because the slowing of  $\tau_{\text{act}}$  was voltage independent,  $\beta$  evidently is negligibly small in the voltage range measured, hence  $\tau_{\text{act}} \approx \alpha^{-1}$ . The opening rate will be slowed by the factor  $(1 - P_{\text{Zn}})$ , where  $P_{\text{Zn}}$  is the probability that the receptor is occupied by  $\text{Zn}^{2+}$  (the occupancy plotted in Fig. 13). Thus the observed time constant will be  $\sim [\alpha (1 - P_{\text{Zn}})]^{-1}$ , and the ratio of  $\tau_{\text{act}}$  in the presence of  $\text{ZnCl}_2$  to that in its absence will be simply  $(1 - P_{\text{Zn}})^{-1}$ . Given these assumptions,  $\tau_{\text{act}}$  is slowed by a factor of 2.0 at the  $K_M$  of  $\text{Zn}^{2+}$ .

In Fig. 11, the  $\tau_{\text{act}}$  data from Fig. 6 are replotted with smooth curves superimposed that assume Model 6, in which the  $\text{Zn}^{2+}$  receptor is formed by three protonation sites and protonation of each site reduces the affinity of the receptor for  $\text{Zn}^{2+}$  by a factor  $a$ . We selected Model 6 because it comes closest to embodying the pH dependence observed. The entire set of theoretical curves is determined by the assumption that a  $\text{Zn}^{2+}$ -bound channel cannot open, and by  $pK_M = 6.5$ ,  $pK_a = 6.3$ , and cooperativity factor  $a = 0.03$ . Setting  $a$  to 0.03 produces an  $\sim 100$ -fold change in apparent  $\text{Zn}^{2+}$  potency between pH 5 and 6 that resembles the  $\tau_{\text{act}}$  data. With  $a = 0.01$ , the shift was too large, and at  $a = 0.1$  the shift was too small. We could not collect data at pH 4, which might have revealed whether the saturation of the effect at very low pH predicted by this model (appendix) occurs. The agreement is generally excellent, although the slope of the data appears shallower than that defined by the theory. Expressed in terms of  $\text{Zn}^{2+}$  activity rather than concentration, calculated with to the Davies equation (Stumm and Morgan, 1981) at the ionic strength of all solutions used,  $\sim 0.13$  M, the  $pK_M$  is 7.0.

### Model of the Interaction between $Zn^{2+}$ and $H^+$ that Shifts the $g_H$ -V Relationship

The effects of  $ZnCl_2$  on the  $g_H$ -V relationship were modeled in a similar manner as the effects on  $\tau_{act}$ . Fig. 12 shows the predictions of Model 6 (as in Fig. 11), with parameters adjusted to match the  $ZnCl_2$  data from Fig. 7, which are superimposed. Several differences in the  $g_H$ -V data compared with the  $\tau_{act}$  data (Fig. 11) required different parameters. It was necessary to assume that more than two protonation sites were involved because the shift between  $pH_o$  6 and 5 was  $\sim 230$ , whereas 100 is the maximum possible shift for a two-site model.  $pK_M$  in all equations is defined by the metal concentration-response relationship at high  $pH_o$ , where binding is unaffected by pH.  $pK_a$  is somewhat model dependent, and is defined by the  $pH_o$  at which the interaction between metal and  $H^+$  saturates. For a given model, this is set by the size of the shift in the high  $pH_o$  region. Thus, in Fig. 12,  $pK_a$  is 7.0 because this produces a sixfold shift between  $pH_o$  8 and 7, as observed in the data. Finally, it was necessary to assume some interaction between binding sites, because pure competition in a three-site model predicts too large a shift at low  $pH_o$ . The value of the interaction factor,  $a$ , is established by the entire shift over the  $pH_o$  range from 8 to 5. This shift was  $10^5$  in the data, and  $a = 0.01$  matched this value. Setting  $a = 0.02$  reduced the range to  $3 \times 10^4$  and at  $a = 0$  (pure competition) the range was too large,  $4 \times 10^5$ . The mechanistic interpretation is that protonation of one of the sites lowers the affinity of the  $Zn^{2+}$  receptor 100-fold. Assuming the same model, the affinity of  $Cd^{2+}$  for the external metal receptor is lower than that of  $Zn^{2+}$  by  $\sim 2$  U (roughly  $pK_M$  6).

A depolarizing shift in the  $g_H$ -V relationship at low  $P_{open}$  can be approximated as a reduction of  $P_{open}$  by a constant fraction. Because the slope factor of the  $g_H$ -V relationship fit by a simple Boltzmann function is  $\sim 10$  mV (DeCoursey and Cherny, 1994; Cherny et al., 1995), an e-fold reduction in  $P_{open}$  should produce a 10-mV depolarizing shift. In Fig. 12, we use Model 6 under the assumption that the channel cannot open when  $Zn^{2+}$  is bound. The voltage shift is given by  $\ln(1 - P_{Zn})^{-1} \times 10$  mV. The  $g_H$ -V data were best described by  $pK_M = 8.0$ ,  $pK_a = 7.0$ , and  $a = 0.01$ . Expressed in terms of  $Zn^{2+}$  activity rather than concentration,  $pK_M$  is 8.5.

The  $g_H$ -V data were best described by  $pK_M = 8.0$ ,  $pK_a = 7.0$ , and  $a = 0.01$  (Fig. 12), whereas the optimal values for the same model of  $\tau_{act}$  data were  $pK_M = 6.5$ ,  $pK_a = 6.3$ , and  $a = 0.03$  (Fig. 11). The different parameter values describing the interactions observed for the  $g_H$ -V relationship and  $\tau_{act}$  may reflect that the former is a steady state parameter and the latter a kinetic one. Alternatively, distinct metal binding sites may be involved in slowing  $\tau_{act}$  and shifting the  $g_H$ -V relationship, as suggested by the greater relative potency of  $ZnCl_2$  (com-

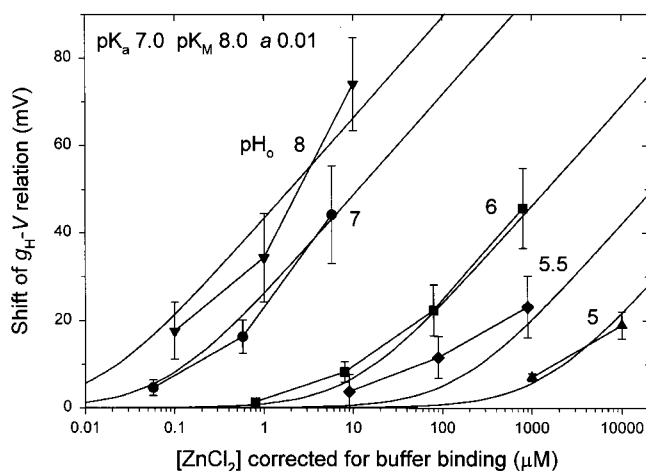


Figure 12. Optimized model predictions for the effect of  $ZnCl_2$  on the  $g_H$ -V relationship (shown in Fig. 7). Eq. A6 is assumed for reasons described in the text, but with somewhat different parameters than in Fig. 11, where the  $\tau_{act}$  effect is modeled:  $pK_M$  is 8.0,  $pK_a$  is 7.0, and  $a = 0.01$ . The model implies that the external  $Zn^{2+}$  receptor consists of three protonation sites, and that protonation of one site reduces the affinity of  $Zn^{2+}$  for the receptor 100-fold.

pared with other metals) for the slowing effect. If so, the “nonspecific” site at which polyvalent metals shift all voltage-dependent parameters simply has a higher  $pK_a$  than the site that regulates  $\tau_{act}$ . Another possibility is that the  $Zn^{2+}$  receptor has a higher affinity for both protons and  $Zn^{2+}$  when the channel is open. This idea is incompatible with the external  $Zn^{2+}$  receptor being comprised of the regulatory protonation sites that govern gating in our model, because these sites become inaccessible to the external solution when the channel is open (Cherny et al., 1995). We saw no evidence of decay of  $H^+$  current in the presence of metals, which would be expected if metals bound (with resolvable kinetics) preferentially to open channels. A final possibility is that fitting the  $\tau_{act}$  and  $g_H$ -V data simply provides two ways to estimate the binding parameters of the  $Zn^{2+}$  receptor.

### Evidence that Metals Bind to the External Site that Regulates pH-Dependent Gating

The modeling exercise indicates that protons and polyvalent cations (at least  $Zn^{2+}$  and  $Cd^{2+}$ ) compete for a common site at the external surface of the  $H^+$  channel. Furthermore, the metal receptor can also bind two or more  $H^+$ , and protonation inhibits metal binding. The best fit was achieved with the assumption that three protonation sites coordinate one  $Zn^{2+}$ . We propose that metal binds to the same external modulatory sites at which extracellular protons regulate the gating of  $H^+$  channels. Extracellular metals and protons have

qualitatively similar effects on channel gating. Both slow activation (increase  $\tau_{\text{act}}$ ), shift the voltage-activation curve ( $g_{\text{H}}-V$  relation) to more positive potentials, and have relatively small effects on the channel closing rate. In our model (Cherny et al., 1995), the  $\Delta\text{pH}$  dependence of gating arises from the requirement that three externally accessible sites must be deprotonated for the channel to open. The agreement between the numbers of protonation sites involved in gating and  $\text{Zn}^{2+}$  binding may be serendipitous, but lends support to both models.

#### *Internal Metal Binding Site*

Although metals produce dramatic effects on  $\text{H}^+$  currents at quite low concentrations for external application, internally applied  $\text{ZnCl}_2$  or  $\text{CdCl}_2$  also altered  $\text{H}^+$  currents. Deactivation was slowed with no effect on  $\tau_{\text{act}}$ , and  $\text{H}^+$  current amplitude was reduced. Because internally applied  $\text{ZnCl}_2$  had relatively weak effects, we could not study them in as much detail, and could not determine whether  $\text{Zn}^{2+}$  and  $\text{H}^+$  compete for internal sites. Nevertheless, in our model (Cherny et al., 1995), the first step in channel closing is deprotonation at internally accessible sites. Thus, the slowing of deactivation by internal  $\text{ZnCl}_2$  with no effect on the opening rate is qualitatively consistent with the idea that  $\text{Zn}^{2+}$  binds to the same internal protonation sites that help regulate gating.

Because the effects of internal and external addition were qualitatively different, distinct metal binding sites must exist at the inner and outer surfaces of the channel. In contrast,  $\text{ZnCl}_2$  has similar effects whether applied externally or internally to  $\text{K}^+$  channels, on ionic currents (Begenisich and Lynch, 1974; Spires and Begenisich, 1992, 1994) as well as on gating currents (Spires and Begenisich, 1995), leading Spires and Begenisich (1995) to conclude that  $\text{Zn}^{2+}$  can reach its binding site in the channel from either side of the membrane. The dissimilarity of effects on  $\text{H}^+$  channels leads us to conclude that there are distinct internal and external sites and, furthermore, that negligible quantities of these metals applied internally reach the external binding site. Not only is there no evidence that  $\text{ZnCl}_2$  can cross the membrane, the lack of effects of  $\text{pH}_i$  on external  $\text{ZnCl}_2$  effects (Fig. 6) indicates that intracellular protons do not affect the local pH near the external  $\text{Zn}^{2+}$  receptor. Thus,  $\text{H}^+$  channels are less promiscuous than are  $\text{K}^+$  channels. In turn, this conclusion supports the concept that voltage-gated proton channels are not water-filled pores that might conduct detectable amounts of  $\text{Zn}^{2+}$  or  $\text{Cd}^{2+}$  (or perhaps  $\text{ZnOH}^+$  or  $\text{CdOH}^+$ ), but instead comprise a hydrogen-bonded chain. The extremely high selectivity of  $\text{H}^+$  channels is another argument for this conduction mechanism (DeCoursey and Cherny, 1994, 1998, 1999a,b).

#### *The Chemical Nature of the Protonation Sites on $\text{H}^+$ Channels*

To account for the  $\Delta\text{pH}$  dependence of the voltage activation curve of the  $\text{H}^+$  channel, we originally proposed identical external and internal protonation sites with  $pK_a$  8.5 (Cherny et al., 1995). Deprotonation at the external site was the first step in channel opening, and deprotonation at the internal site was the first step in channel closing. That deuterium substitution slowed activation threefold with negligible effects on closing suggested that the external and internal sites were chemically different, with the external site likely composed of His, Lys, or Tyr residues and the internal site possibly a sulfhydryl group, presumably Cys (DeCoursey and Cherny, 1997). A classical example of His forming a Zn-binding site is carbonic anhydrase, in which zinc is coordinated between three His residues (and one  $\text{OH}^-$ ) to form the catalytic site of this metalloenzyme (Silverman and Vincent, 1983). Chelators can remove this zinc and it can then be replaced by various other ligands, which bind with a relative potency  $\text{Hg} \gg \text{Cu} > \text{Zn} > \text{Cd}, \text{Ni} > \text{Co} > \text{Mn}$  (Silverman and Vincent, 1983), a sequence similar to that reported for metal inhibition of  $\text{H}^+$  currents (see above). The data presented here are compatible with the idea that the  $\text{Zn}^{2+}$  binding site is the same site at which external protons regulate gating. In this regard, it is intriguing that  $\text{pH}_o$  acting on extracellular His residues shifts the voltage dependence of the gating of a plant  $\text{K}^+$  channel (Hoth et al., 1997). Protonation of this stomatal guard cell channel shifts the activation curve toward more positive voltages, just as the  $g_{\text{H}}-V$  relation of voltage-gated proton channels is shifted to the right at lower  $\text{pH}_o$ . Because this  $\text{K}^+$  channel is activated by hyperpolarization, it is activated by low  $\text{pH}_o$ , whereas the voltage-gated proton channel is activated by depolarization and thus is inhibited by low  $\text{pH}_o$ . Zinc binding sites have been created in  $\alpha$ -hemolysin channels by introducing His residues (Walker et al., 1994; Kasianowicz et al., 1999). The external  $\text{Zn}^{2+}$  receptor on  $\text{H}^+$  channels binds  $\text{Zn}^{2+}$  with a substantially higher affinity,  $pK_M \sim 6.5$ , than the "normal" association constant for 1:1 binding of Zn(II) to His,  $pK_M$  2.5 (Breslow, 1973). The higher affinity is compatible with our conclusion that multiple His (or other ionizable groups) coordinate the binding of a single  $\text{Zn}^{2+}$ . The  $\text{Zn}^{2+}$  dissociation constant for carbonic anhydrase, in which three His coordinate one  $\text{Zn}^{2+}$ , is 4 pM (Kiefer et al., 1993). The typical  $pK_a$  of His in proteins ranges from 6.4 to 7.2 (Breslow, 1973), encompassing the  $pK_a$  values derived from most of the models tested here. Thus, many types of evidence point to His as a likely candidate for forming the external  $\text{Zn}^{2+}$  receptor.

Henderson (1998) demonstrated recently that mutation of any of three His residues to Leu in a putative

transmembrane domain abolished the H<sup>+</sup> conductance associated with NADPH oxidase in neutrophils. This intriguing result may support the identity of the external modulatory site as His. However, epithelial and phagocyte H<sup>+</sup> channels differ significantly (DeCoursey, 1998), and some phagocyte H<sup>+</sup> channels have a higher sensitivity to ZnCl<sub>2</sub> (Bánfi et al., 1999). Furthermore, the role of one or more of the His might be in conduction, forming part of the hydrogen-bonded chain, rather than in regulation of gating.

The much weaker deuterium isotope effect on H<sup>+</sup> channel closing than on opening led to the suggestion of Cys as a candidate for the internal regulatory protonation site because sulfhydryl groups typically have smaller *pK<sub>a</sub>* shifts in D<sub>2</sub>O (DeCoursey and Cherny, 1997). The weak effects of internal ZnCl<sub>2</sub> reported here, however, must be reconciled with the typically high affinity binding of Zn<sup>2+</sup> to Cys (Breslow, 1973). If Cys does help form the internal site, steric constraints may allow proton or deuteron binding, but disfavor close approach by Zn<sup>2+</sup>.

### Pathophysiological Significance

Because they are more sensitive to polyvalent metal cations than most other ion channels, H<sup>+</sup> channels would be among the first to register effects of metal poisoning. Human plasma zinc levels are maintained at ~15 μM (Cornelis and Versieck, 1980), most of which is complexed with plasma proteins or phosphates. However, the *g<sub>H</sub>*-V relationship is quite sensitive to Zn<sup>2+</sup> at physiological pH with a distinct shift at <0.1 μM ZnCl<sub>2</sub> (Fig. 7). ZnCl<sub>2</sub> or CdCl<sub>2</sub> suppress the respiratory burst—the release of bactericidal reactive oxygen species—in human neutrophils in vitro, presumably by inhibiting H<sup>+</sup> currents (Henderson et al., 1988). Inhalation of zinc oxide produces metal fume fever, apparently by elevating plasma interleukin-6 (a pyrogen produced by granulocytes) levels (Fine et al., 1997). Voltage-gated proton channels in alveolar epithelium may contribute to CO<sub>2</sub> extrusion by the lung (DeCoursey, 2000). Volume regulation of alveolar epithelial cells is inhibited by high concentrations of ZnCl<sub>2</sub> (Jones et al., 1982). This evidence is circumstantial, but worth worrying about.

### APPENDIX

#### Competition between Zn<sup>2+</sup> and H<sup>+</sup>

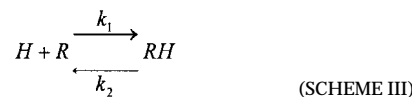
If Zn<sup>2+</sup> is the sole form of ZnCl<sub>2</sub> active on H<sup>+</sup> channels, then the strong pH<sub>0</sub> sensitivity of its effects (Figs. 5–6) could be explained in two ways. Zn<sup>2+</sup> and H<sup>+</sup> might compete for the same site on the channel, or protonation of the channel might lower its affinity for Zn<sup>2+</sup>. Several classes of mechanisms encompassing both possibilities can be envisioned. Here we will explore the ex-

tent to which the stoichiometry of the apparent competition between metal and protons defines the nature of the metal receptor. To make this analysis as model-independent as possible, we will simply consider the probability that Zn<sup>2+</sup> is bound to its receptor. In the discussion we assumed specific mechanisms by which metals slow H<sup>+</sup> channel activation (Fig. 11) or shift the *g<sub>H</sub>*-V relationship (Fig. 12), and determine the model parameters given those assumptions.

If one Zn<sup>2+</sup> (*M*) competes with one H<sup>+</sup> (*H*) for the same binding site or receptor (*R*), each will have a dissociation constant, defined in Schemes II and III, respectively (the brackets indicating concentration have been omitted):



and



as  $K_M = k_b/k_f$  and  $K_a = k_2/k_1$ .

We define  $pK_M$  the way  $pK_a$  is defined, as the negative logarithm of  $K_M$ . Note that  $K_M$  as defined here is the inverse of the metal-buffer binding constant defined by Good et al. (1966), thus we indicate their parameter as  $K'_M$  (Table I). The fraction of channels with metal bound to them is given by a “simple competition” model:

$$\frac{RM}{R + RM + RH} = \frac{1}{1 + \frac{K_M}{M} \left(1 + \frac{H}{K_a}\right)}, \quad (\text{A1})$$

where the number of free, metal-bound, or protonated receptors is *R*, *RM*, or *RH*, respectively (see Spires and Begenisich, 1992). Eq. A1, illustrated in Fig. 13 A, predicts that, well below the *pK<sub>a</sub>*, the apparent potency of metal will decrease 10-fold per unit decrease in pH (Clark, 1926). An example in which such a relationship holds is the affinity of zinc for the *bc*<sub>1</sub> complex, which decreases 10-fold per unit decrease in pH between pH 7 and 5 (Link and von Jagow, 1995). Eq. A1 agrees with the ~10-fold reduction in potency seen between pH<sub>0</sub> 7 and 6, but the decrease in apparent potency of Zn<sup>2+</sup> between pH<sub>0</sub> 6 and 5 is closer to 100-fold (Fig. 6). Therefore, this model must be abandoned.

We next consider noncompetitive inhibition, in which Zn<sup>2+</sup> and H<sup>+</sup> bind independently to different sites, and the effect is observed only when Zn<sup>2+</sup> and not H<sup>+</sup> is bound. This “noncompetitive inhibition” model is:

$$\frac{RM}{R + RM + RH + RMH} = \frac{1}{\left(1 + \frac{K_M}{M}\right) \left(1 + \frac{H}{K_a}\right)}. \quad (\text{A2})$$

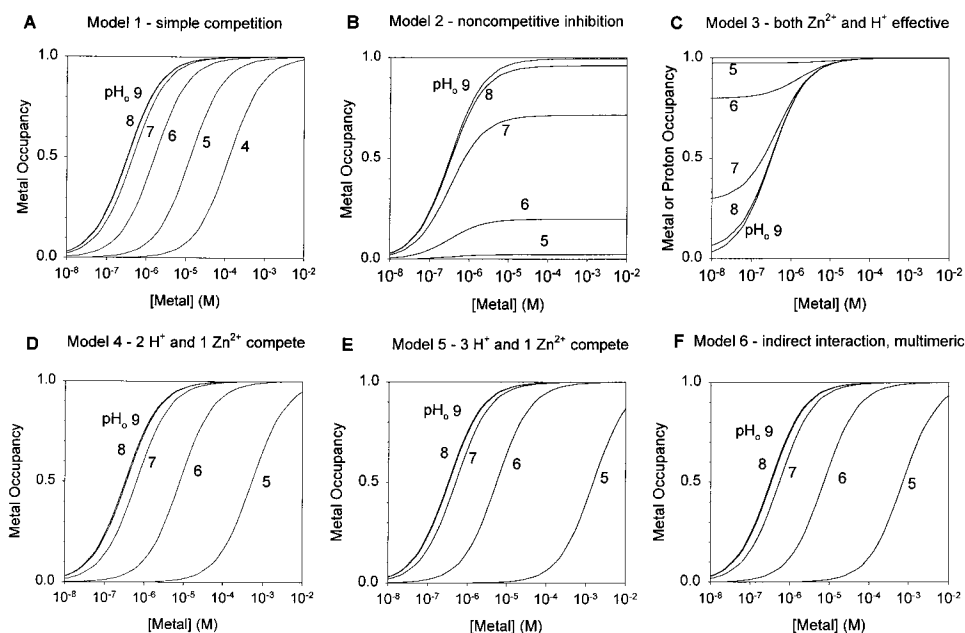


Figure 13. The probability that the metal receptor is occupied by a metal ion as predicted by various models with different assumptions about the interaction between  $H^+$  and  $Zn^{2+}$ . To relate the occupancy of the metal receptor to data such as in Fig. 6, it is necessary to assume a specific mechanism, as discussed in the text. On the other hand, the  $pK_a$  value is set by the  $pH_0$  at which the effect saturates, and is relatively insensitive to this relationship. Binding constants for  $H^+$  and  $Zn^{2+}$ ,  $pK_a$ , and  $pK_M$ , respectively, are defined in the text. (A) Model 1 ( $pK_a$  6.6 and  $pK_M$  6.5, from Eq. A1) assumes simple competition between  $H^+$  and  $Zn^{2+}$  for a single site. At low pH, the concentration of  $Zn^{2+}$  required to produce a given occupancy increases 10-fold per unit decrease in pH. (B) Model 2

( $pK_a$  6.6 and  $pK_M$  6.5, from Eq. A2) describes noncompetitive inhibition, in which  $H^+$  and  $Zn^{2+}$  bind independently to separate sites. These curves superimpose if scaled up. (C) Model 3 ( $pK_a$  6.6 and  $pK_M$  6.5, from Eq. A3) assumes that the effect is the same whether  $H^+$  or  $Zn^{2+}$  is bound to the site. If the pH 5 curve is scaled to the pH 9 curve, the former is shifted to the right  $\sim 10$ -fold. (D) Model 4 ( $pK_a$  6.6 and  $pK_M$  6.5, from Eq. A4) assumes two identical protonation sites that combine to coordinate one  $Zn^{2+}$  ion. Pure competition is assumed, in that protonation of either site prevents  $Zn^{2+}$  binding. (E) Model 5 ( $pK_a$  6.2 and  $pK_M$  6.5, from Eq. A5) is identical to Model 4 except that there are three independent sites, protonation of any of which prevents  $Zn^{2+}$  binding. The  $pK_a$  was adjusted to reproduce the 10-fold change in apparent potency of  $Zn^{2+}$  observed between pH 6 and 7 (Fig. 6), but the apparent potency of  $Zn^{2+}$  changes too much between pH 6 and 5 ( $\sim 285$ -fold, compared with 100-fold for the data in Fig. 6), and  $\sim 850$ -fold between pH 5 and 4, approaching the low pH limit of a 1,000-fold change. (F) Model 6 ( $pK_a$  6.3,  $pK_M$  6.5, and  $a = 0.03$ , from Eq. A6) assumes three sites, but the protonation of one site lowers the affinity of the next site(s) to 0.03 of the original affinity. In essence, the fully protonated channel has a much lower affinity for  $Zn^{2+}$  (apparent  $pK_M \sim 1.3$ ) so that the effect of pH on  $Zn^{2+}$  saturates at either high or low pH. With this interaction factor ( $a = 0.03$ ), decreasing pH from 4 to 3 lowers the  $Zn^{2+}$  affinity less than twofold, and lowering pH to  $< 3$  has no further effect.

In Eq. A2, metal simply becomes ineffective at low pH (Fig. 13 B). Furthermore, the “threshold” concentration of metal is the same at all pH. In contrast, the data exhibit large effects of  $Zn^{2+}$  at low  $pH_0$ , where the concentration–response relationship appears simply to shift to higher  $[Zn^{2+}]$  (Figs. 5 and 6). Furthermore, the threshold concentration that produces detectable effects changes radically with pH. Therefore, we rule out purely noncompetitive models.

The simple competition model could be altered to reflect that  $Zn^{2+}$  and  $H^+$  have qualitatively similar effects when bound to  $H^+$  channels. Both cations slow activation at a given voltage, and shift the voltage-activation curve to more positive potentials. The formulation of this “both  $Zn^{2+}$  and  $H^+$  effective” model is (Eq. A3):

$$\frac{RM + RH}{R + RM + RH} = \frac{\frac{M}{K_M} + \frac{H}{K_a}}{1 + \frac{M}{K_M} + \frac{H}{K_a}} \quad (A3)$$

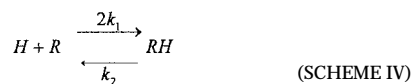
As is apparent from Fig. 13 C, if there is competitive binding and  $Zn^{2+}$  and  $H^+$  have the same effects, then

at low  $pH_0$  there will be little further effect of adding metal because all the sites are already protonated. There is a small shift of the threshold  $[Zn^{2+}]$ , but this occurs at the expense of reducing the maximal effect. At least this simple form of the “both effective” class of models is incompatible with the data.

A more complicated model is necessary to explain the  $\sim 100$ -fold shift in apparent potency of  $Zn^{2+}$  between  $pH_0$  6 and 5. One possibility is that each channel has multiple protonation sites near enough to each other that two can coordinate a single  $Zn^{2+}$ . The divalency of  $Zn^{2+}$  suggests this idea naturally. A channel that coordinates  $Zn^{2+}$  between His and Asp side groups has been described (Kasianowicz et al., 1999). We model this possibility by assuming that the  $Zn^{2+}$  receptor can bind two protons. Protonation of either site prevents  $Zn^{2+}$  binding. The metal occupancy will be given by Eq. A4 (2  $H^+$  and 1  $Zn^{2+}$  compete):

$$\frac{RM}{R + RM + RH + RH_2} = \frac{1}{1 + \frac{K_M}{M} \left[ 1 + \frac{H}{K_a} \left( 2 + \frac{H}{K_a} \right) \right]} \quad (A4)$$

assuming that the two protonation sites are identical and independent. Here  $K_a = k_2/k_1$ , with  $k_1$  and  $k_2$  defined in the two partial reactions of the degenerate two-step system (Bernasconi, 1976) (Schemes IV and V):



and

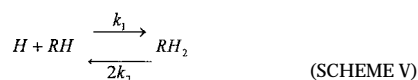


Fig. 13 D shows the prediction of Eq. A4, assuming that  $pK_a = 6.6$  and  $pK_M = 6.5$ . The values of  $pK_a$  and  $pK_M$  are established from the pH range at which the  $pH_0$  sensitivity of  $Zn^{2+}$  diminishes, and from the position of the concentration–response curve at high  $pH_0$ , respectively. In Eq. A4, the apparent efficacy of  $Zn^{2+}$  decreases 100-fold/U at low  $pH_0$ , consistent with the shift observed between pH 6 and 5. The equation describes the  $\tau_{act}$  data (Fig. 6) fairly well, although the calculated shift between pH 6 and 5 is only 70 rather than 100, because the low  $pH_0$  behavior is not fully manifest at these relatively high  $pH_0$ . It might be expected that protonation of the first site would lower the proton affinity of the second site. We modeled this by lowering the  $pK_a$  of the second protonation reaction, but there were only subtle differences in the predicted behavior for two sites with identical  $pK_a$  compared with two sites with 1 U different  $pK_a$  having the same average value.

If the  $H^+$  channel were a trimer or tetramer, there might reasonably be three or four equivalent protonation sites. Assuming that protonation of any site prevents metal binding, this purely competitive model is described by (see Perez-Cornejo et al., 1998):

$$\text{Metal occupancy} = \frac{1}{1 + \frac{K_M}{M} \left(1 + \frac{H}{K_a}\right)^n} \quad (\text{A5})$$

In Eq. A5, the shift in apparent  $Zn^{2+}$  potency at low  $pH_0$  is  $10^3$  for  $n = 3$  and  $10^4$  for  $n = 4$ . Although the data do not exhibit a shift that large, the three-site Model 5 (Fig. 13 E, “ $H^+$  and 1  $Zn^{2+}$  compete”) can simulate the data tolerably well using  $pK_a$  6.2 and  $pK_M$  6.5 because the 1,000-fold/U shift is attained only at lower pH than the range of the data.

One final variant will be considered, in which the channel has multiple protonation sites that interfere with  $Zn^{2+}$  binding, either allosterically or electrostatically. Protonation of each successive site lowers the affinity of the metal binding site for  $Zn^{2+}$ , but protonation and  $Zn^{2+}$  binding are not mutually exclusive. The general “indirect interaction, multimeric site” model is (Perez-Cornejo et al., 1998):

$$\text{Metal occupancy} = \frac{\left(1 + a \frac{H}{K_a}\right)^n}{\left(1 + a \frac{H}{K_a}\right)^n + \frac{K_M}{M} \left(1 + a \frac{H}{K_a}\right)^n} \quad (\text{A6})$$

where factor  $a$  is a cooperativity factor that is unity for completely independent binding of  $H^+$  and  $Zn^{2+}$ , decreases as the metal affinity is reduced, and becomes 0 when there is pure competition (in which case Eq. A6 reduces to Eq. A5). This model behaves as though, in the limit of high and low pH, the affinity of the site for  $Zn^{2+}$  is high or low, respectively. Thus, the shift in apparent metal potency saturates at both high and low pH in contrast with purely competitive Models 1, 4, and 5 (Fig. 13), which saturate at high pH only.

The authors are indebted to Tatiana Iastrebova for her meticulous measurements of metal binding affinity to buffers and her technical assistance. The authors appreciate helpful criticism and preprints from Ted Begenisich, John J. Kasianowicz, and Vladislav S. Markin.

This work was supported in part by research grant HL52671 to Dr. DeCoursey from the National Institutes of Health.

Submitted: 4 October 1999 Revised: 8 November 1999 Accepted 8 November 1999 Released online: 29 November 1999

## REFERENCES

- Arkett, S.A., S.J. Dixon, and S.M. Sims. 1994. Effects of extracellular calcium and protons on osteoclast potassium currents. *J. Membr. Biol.* 140:163–171.
- Arslan, P., F. Di Virgilio, M. Beltrame, R.Y. Tsien, and T. Pozzan. 1985. Cytosolic  $Ca^{2+}$  homeostasis in Ehrlich and Yoshida carcinomas: a new, membrane-permeant chelator of heavy metals reveals that these ascites tumor cell lines have normal cytosolic free  $Ca^{2+}$ . *J. Biol. Chem.* 260:2719–2727.
- Baes, C.F., and R.E. Mesmer. 1976. *The Hydrolysis of Cations*. John Wiley & Sons Inc., New York, NY. 489 pp.
- Bánfi, B., J. Schrenzel, O. Nüsse, D.P. Lew, E. Ligeti, K.-H. Krause, and N. Demaurex. 1999. A novel  $H^+$  conductance in eosinophils: unique characteristics and absence in chronic granulomatous disease. *J. Exp. Med.* 190:183–194.
- Barish, M.E., and C. Baud. 1984. A voltage-gated hydrogen ion current in the oocyte membrane of the axolotl, *Ambystoma*. *J. Physiol.* 352:243–263.
- Begenisich, T., and C. Lynch. 1974. Effects of internal divalent cations on voltage-clamped squid axons. *J. Gen. Physiol.* 63:675–689.
- Bernasconi, C.F. 1976. *Relaxation Kinetics*. Academic Press, Inc., New York, NY. 288 pp.
- Bernheim, L., R.M. Krause, A. Baroffio, M. Hamann, A. Kaelin, and C.-R. Bader. 1993. A voltage-dependent proton current in cultured human skeletal muscle myotubes. *J. Physiol.* 470:313–333.

- Breslow, E. 1973. Metal-protein complexes. *In Inorganic Biochemistry*. Vol. 1. G.L. Eichhorn, editor. Elsevier Scientific Publishing Co., Amsterdam, Netherlands. 227–249.
- Byerly, L., R. Meech, and W. Moody. 1984. Rapidly activating hydrogen ion currents in perfused neurones of the snail, *Lymnaea stagnalis*. *J. Physiol.* 351:199–216.
- Byerly, L., and Y. Suen. 1989. Characterization of proton currents in neurones of the snail, *Lymnaea stagnalis*. *J. Physiol.* 413:75–89.
- Cherny, V.V., V.S. Markin, and T.E. DeCoursey. 1995. The voltage-activated hydrogen ion conductance in rat alveolar epithelial cells is determined by the pH gradient. *J. Gen. Physiol.* 105:861–896.
- Clark, A.J. 1926. The antagonism of acetyl choline by atropine. *J. Physiol.* 61:547–556.
- Cole, K.S., and J.W. Moore. 1960. Potassium ion current in the squid giant axon: dynamic characteristic. *Biophys. J.* 1:1–14.
- Cornelis, R., and J. Versieck. 1980. Critical evaluation of the literature values of eighteen trace elements in human serum or plasma. *In: Trace Element Analytical Chemistry in Medicine and Biology*. P. Brätter and P. Schramel, editors. Walter de Gruyter, Berlin, Germany. 587–600.
- DeCoursey, T.E. 1990. State-dependent inactivation of K<sup>+</sup> currents in rat type II alveolar epithelial cells. *J. Gen. Physiol.* 95:617–646.
- DeCoursey, T.E. 1991. Hydrogen ion currents in rat alveolar epithelial cells. *Biophys. J.* 60:1243–1253.
- DeCoursey, T.E. 1998. Four varieties of voltage-gated proton channels. *Front. Biosci.* 3:d477–d482.
- DeCoursey, T.E. 2000. Hypothesis: do voltage-gated H<sup>+</sup> channels in alveolar epithelial cells contribute to CO<sub>2</sub> elimination by the lung? *Am. J. Physiol. Cell Physiol.* In press.
- DeCoursey, T.E., and V.V. Cherny. 1993. Potential, pH, and arachidonate gate hydrogen ion currents in human neutrophils. *Biophys. J.* 65:1590–1598.
- DeCoursey, T.E., and V.V. Cherny. 1994. Voltage-activated hydrogen ion currents. *J. Membr. Biol.* 141:203–223.
- DeCoursey, T.E., and V.V. Cherny. 1995. Voltage-activated proton currents in membrane patches of rat alveolar epithelial cells. *J. Physiol.* 489:299–307.
- DeCoursey, T.E., and V.V. Cherny. 1996. II. Voltage-activated proton currents in human THP-1 monocytes. *J. Membr. Biol.* 152:131–140.
- DeCoursey, T.E. and V.V. Cherny. 1997. Deuterium isotope effects on permeation and gating of proton channels in rat alveolar epithelium. *J. Gen. Physiol.* 109:415–434.
- DeCoursey, T.E., and V.V. Cherny. 1998. Temperature dependence of voltage-gated H<sup>+</sup> currents in human neutrophils, rat alveolar epithelial cells, and mammalian phagocytes. *J. Gen. Physiol.* 112:503–522.
- DeCoursey, T.E., and V.V. Cherny. 1999a. An electrophysiological comparison of voltage-gated proton channels, other ion channels, and other proton channels. *Isr. J. Chem.* In press.
- DeCoursey, T.E., and V.V. Cherny. 1999b. Common themes and problems of bioenergetics and voltage-gated proton channels. *Biochim. Biophys. Acta*. In press.
- DeCoursey, T.E., E.R. Jacobs, and M.R. Silver. 1988. Potassium currents in rat type II alveolar epithelial cells. *J. Physiol.* 395:487–505.
- Demaurex, N., S. Grinstein, M. Jaconi, W. Schlegel, D.P. Lew, and K.-H. Krause. 1993. Proton currents in human granulocytes: regulation by membrane potential and intracellular pH. *J. Physiol.* 466:329–344.
- Eder, C., H.-G. Fischer, U. Hadding, and U. Heinemann. 1995. Properties of voltage-gated currents of microglia developed using macrophage colony-stimulating factor. *Pflügers Arch.* 430:526–533.
- Eigen, M., and G.G. Hammes. 1963. Elementary steps in enzyme reactions (as studied by relaxation spectrometry). *Adv. Enzymol.* 25:1–38.
- Fine, J.M., T. Gordon, L.C. Chen, P. Kinney, G. Falcone, and W.S. Beckett. 1997. Metal fume fever: characterization of clinical and plasma IL-6 responses in controlled human exposures to zinc oxide fume at and below the threshold limit value. *J. Occup. Environ. Med.* 39:722–726.
- Frankenhaeuser, B., and A.L. Hodgkin. 1957. The action of calcium on the electrical properties of squid axons. *J. Physiol.* 137:218–244.
- Gilly, W.F., and C.M. Armstrong. 1982. Divalent cations and the activation kinetics of potassium channels in squid giant axons. *J. Gen. Physiol.* 79:965–996.
- Good, N.E., G.D. Winget, W. Winter, T.N. Connolly, S. Izawa, and R.M.M. Singh. 1966. Hydrogen ion buffers for biological research. *Biochemistry.* 5:467–477.
- Gordienko, D.V., M. Tare, S. Parveen, C.J. Fenech, C. Robinson, and T.B. Bolton. 1996. Voltage-activated proton current in eosinophils from human blood. *J. Physiol.* 496:299–316.
- Henderson, L.M. 1998. Role of histidines identified by mutagenesis in the NADPH oxidase-associated H<sup>+</sup> channel. *J. Biol. Chem.* 273:33216–33223.
- Henderson, L.M., J.B. Chappell, and O.T.G. Jones. 1988. Superoxide generation by the electrogenic NADPH oxidase of human neutrophils is limited by the movement of a compensating charge. *Biochem. J.* 255:285–290.
- Hille, B. 1968. Charges and potentials at the nerve surface: divalent ions and pH. *J. Gen. Physiol.* 51:221–236.
- Hille, B., and W. Schwarz. 1978. Potassium channels as multi-ion single-file pores. *J. Gen. Physiol.* 72:409–442.
- Hoth, S., I. Dreyer, P. Dietrich, D. Becker, and B. Müller-Röber. 1997. Molecular basis of plant-specific acid activation of K<sup>+</sup> uptake channels. *Proc. Natl. Acad. Sci. USA.* 94:4806–4810.
- Humez, S., F. Fournier, and P. Guilbault. 1995. A voltage-dependent and pH-sensitive proton current in *Rana esculenta* oocytes. *J. Membr. Biol.* 147:207–215.
- Hutter, O.F., and A.E. Warner. 1967. Action of some foreign cations and anions on the chloride permeability of frog muscle. *J. Physiol.* 189:445–460.
- Jones, G.S., P.R. Miles, R.C. Lantz, D.E. Hinton, and V. Castranova. 1982. Ionic content and regulation of cellular volume in rat alveolar type II cells. *J. Appl. Physiol. Respir. Environ. Exerc. Physiol.* 53:258–266.
- Kapus, A., R. Romanek, A.Y. Qu, O.D. Rotstein, and S. Grinstein. 1993. A pH-sensitive and voltage-dependent proton conductance in the plasma membrane of macrophages. *J. Gen. Physiol.* 102:729–760.
- Kasianowicz, J.J., D.L. Burden, L.C. Han, S. Cheley, and H. Bayley. 1999. Genetically engineered metal ion binding sites on the outside of a channel's transmembrane  $\beta$ -barrel. *Biophys. J.* 76:837–845.
- Kiefer, L.L., J.F. Krebs, S.A. Paterno, and C.A. Fierke. 1993. Engineering a cysteine ligand into the zinc binding site of human carbonic anhydrase II. *Biochemistry.* 32:9896–9900.
- Kwan, Y.W., and R.S. Kass. 1993. Interactions between H<sup>+</sup> and Ca<sup>2+</sup> near cardiac L-type calcium channels: evidence for independent channel-associated binding sites. *Biophys. J.* 65:1188–1195.
- Lide, D.R. 1995. CRC Handbook of Chemistry and Physics. CRC Press, Boca Raton, FL. 8.58.
- Link, T.A., and G. von Jagow. 1995. Zinc ions inhibit the Q<sub>p</sub> center of bovine heart mitochondrial bc<sub>1</sub> complex by blocking a protonatable group. *J. Biol. Chem.* 270:25001–25006.
- Mahaut-Smith, M. 1989. The effect of zinc on calcium and hydrogen ion currents in intact snail neurones. *J. Exp. Biol.* 145:455–464.

- Meech, R.W., and R.C. Thomas. 1987. Voltage-dependent intracellular pH in *Helix aspersa* neurones. *J. Physiol.* 390:433–452.
- Nagle, J.F., and H.J. Morowitz. 1978. Molecular mechanisms for proton transport in membranes. *Proc. Natl. Acad. Sci. USA.* 75: 298–302.
- Nordström, T., O.D. Rotstein, R. Romanek, S. Asotra, J.N.M. Heersche, M.F. Manolson, G.F. Brisseau, and S. Grinstein. 1995. Regulation of cytoplasmic pH in osteoclasts: contribution of proton pumps and a proton-selective conductance. *J. Biol. Chem.* 270: 2203–2212.
- Perez-Cornejo, P., P. Stampe, and T. Begenisich. 1998. Proton probing of the charybdotoxin binding site of *Shaker* K<sup>+</sup> channels. *J. Gen. Physiol.* 111:441–450.
- Perrin, D.D., and B. Dempsey. 1974. Buffers for pH and Metal Ion Control. Chapman and Hall, London, UK. 175 pp.
- Robinson, R.A., and R.H. Stokes. 1959. Electrolyte Solutions. Butterworths, London, UK. 571 pp.
- Rychkov, G.Y., D.St.J. Astill, B. Bennetts, B.P. Hughes, A.H. Bretag, and M.L. Roberts. 1997. pH-dependent interactions of Cd<sup>2+</sup> and a carboxylate blocker with the rat ClC-1 chloride channel and its R304E mutant in the Sf-9 insect cell line. *J. Physiol.* 501:355–362.
- Silverman, D.N., and S.H. Vincent. 1983. Proton transfer in the catalytic mechanism of carbonic anhydrase. *CRC Crit. Rev. Biochem.* 14:207–235.
- Spalding, B.C., P. Taber, J.G. Swift, and P. Horowicz. 1990. Zinc inhibition of chloride efflux from skeletal muscle of *Rana pipiens* and its modification by external pH and chloride activity. *J. Membr. Biol.* 116:195–214.
- Spires, S., and T. Begenisich. 1992. Chemical properties of the divalent cation binding site on potassium channels. *J. Gen. Physiol.* 100:181–193.
- Spires, S., and T. Begenisich. 1994. Modulation of potassium channel gating by external divalent cations. *J. Gen. Physiol.* 104:675–692.
- Spires, S., and T. Begenisich. 1995. Voltage-independent gating transitions in squid axon potassium channels. *Biophys. J.* 68:491–500.
- Stanfield, P.R. 1975. The effect of zinc ions on the gating of the delayed potassium conductance of frog sartorius muscle. *J. Physiol.* 251:711–735.
- Stumm, W., and J.J. Morgan. 1981. Aquatic Chemistry: An Introduction Emphasizing Chemical Equilibria in Natural Waters. John Wiley & Sons, New York, NY. 780 pp.
- Thomas, R.C., and R.W. Meech. 1982. Hydrogen ion currents and intracellular pH in depolarized voltage-clamped snail neurones. *Nature.* 299:826–828.
- Walker, B., J. Kasianowicz, M. Krishnaswamy, and H. Bayley. 1994. A pore-forming protein with a metal-actuated switch. *Prot. Eng.* 7:655–662.
- Woodhull, A.M. 1973. Ionic blockage of sodium channels in nerve. *J. Gen. Physiol.* 61:687–708.